Gondwana Research 25 (2014) 1469–1483

Contents lists available at ScienceDirect

Gondwana Research

journal homepage: www.elsevier.com/locate/gr

$^{40}Ar/^{39}Ar$ geochronological constraints on the formation of the Dayingezhuang gold deposit: New implications for timing and duration of hydrothermal activity in the Jiaodong gold province, China

Li-Qiang Yang [a,*], Jun Deng [a], Richard J. Goldfarb [a,b], Jing Zhang [a], Bang-Fei Gao [c], Zhong-Liang Wang [a]

[a] State Key Laboratory of Geological Processes and Mineral Resources, China University of Geosciences, Beijing 100083, China
[b] U.S. Geological Survey, P.O. Box 25046, Denver Federal Center, Denver, CO 80225, USA
[c] China Railway Resources Mineral Exploration Company, Beijing 100039, China

ARTICLE INFO

Article history:
Received 22 April 2013
Received in revised form 20 June 2013
Accepted 5 July 2013
Available online 16 July 2013

Handling Editor: M. Santosh

Keywords:
Dayingezhuang
Orogenic gold
Geochronology
Linglong MCC
Jiaodong, China

ABSTRACT

China's largest gold resource is located in the highly endowed northwestern part of the Jiaodong gold province. Most gold deposits in this area are associated with the NE- to NNE-trending shear zones on the margins of the 130–126 Ma Guojialing granite. These deposits collectively formed at ca. 120 ± 5 Ma during rapid uplift of the granite. The Dayingezhuang deposit is a large (>120 t Au) orogenic gold deposit in the same area, but located along the eastern margin of the Late Jurassic Linglong Metamorphic Core Complex. New $^{40}Ar/^{39}Ar$ geochronology on hydrothermal sericite and muscovite from the Dayingezhuang deposit indicate the gold event is related to evolution of the core complex at 130 ± 4 Ma and is the earliest important gold event that is well-documented in the province. The Dayingezhuang deposit occurs along the Linglong detachment fault, which defines the eastern edge of the ca. 160–150 Ma Linglong granite–granodiorite massif. The anatectic rocks of the massif were rapidly uplifted, at rates of at least 1 km/m.y. from depths of 25–30 km, to form the metamorphic core complex. The detachment fault, with Precambrian metamorphic basement rocks in the hangingwall and the Linglong granitoids and migmatites in the footwall, is characterized by early mylonitization and a local brittle overprinting in the footwall. Gold is associated with quartz–sericite–pyrite–K-feldspar altered footwall cataclasites at the southernmost area of the brittle deformation along the detachment fault. Our results indicate that there were two successive, yet distinct gold-forming tectonic episodes in northwestern Jiaodong. One event first reactivated the detachment fault along the edge of the Linglong massif between 134 and 126 Ma, and then a second reactivated the shears along the margins of the Guojialing granite. Both events may relate to a component of northwest compression after a middle Early Cretaceous shift from regional NW–SE extension to a NE–SW extensional regime.

1. Introduction

Understanding temporal relationships within metallogenic epochs has been a key issue of interest to economic geologists during the past few decades. Determination of the duration of ore-forming events is of major importance for a thorough understanding of the genesis of ore deposits and for identifying associated geological events, such as defining the relationship between ore formation and evolving continental dynamics. Reconstruction of the spatial and temporal patterns of the geologic evolution of many large metallogenic provinces can be complex when characterized by relatively long-lived hydrothermal activity.

The Jiaodong gold province is the area of the most extensive past gold mining and largest recognized gold resources in China. The majority of the production and resources for the province is located in the Zhaoyuan region in the northwestern part of the peninsula (Qiu et al., 2002). Reliable production and resource data for the province, as with gold districts throughout China, are lacking. Based upon various reported accounts, it is likely that the Zhaoyuan region originally contained in excess of 1000 tonnes of Au (t Au). Dozens of operations now produce about 3–5 t Au/year from underground operations. Future large-scale mining development, perhaps with significant open-pit operations, is likely to highlight the brownfields potential that still remains in the region for even a larger resource. Despite the unique tectonic setting of the Jiaodong gold deposits

* Corresponding author at: State Key Laboratory of Geological Processes and Mineral Resources, China University of Geosciences, 29# Xue-Yuan Road, Haidian District, Beijing 100083, China. Tel.: +86 10 8232 1937 (O); fax: +86 10 8232 2175.
E-mail addresses: lqyang@cugb.edu.cn (L.-Q. Yang), goldfarb@usgs.gov (R.J. Goldfarb).

1342-937X © 2013 The Authors. Published by Elsevier B.V. on behalf of International Association for Gondwana Research. Open access under CC BY-NC-ND license.
http://dx.doi.org/10.1016/j.gr.2013.07.001

that has led some workers to define these as a new type of gold deposit (e.g., Zhai and Santosh, 2013), the spatial association with large fault zones, local structural controls, temporal association with uplift, mineral assemblages, alteration, and ore fluid chemistries suggest these are best classified as orogenic gold deposits.

The geochronology of gold mineralization in the Jiaodong gold province has been addressed in many detailed studies during the past decade. A relatively young age for these gold deposits hosted in Precambrian terranes has been recognized for many years now. However, debate still exists (e.g., Li et al., 2006) as to whether these formed during a single event during the Yanshanian (Early Cretaceous) orogen (Wang et al., 1998; Zhou and Lu, 2000; Qiu et al., 2002), or as multiple, late Mesozoic hydrothermal episodes (Deng et al., 1999, 2003; Mao et al., 2003). There are, furthermore, still significant controversies regarding the overall duration of the main orogenic gold deposition event(s) (Wang et al., 2002; Deng et al., 2003; Chen et al., 2005).

Numerous published absolute age constraints of variable quality characterize the gold deposits of the Jiaodong Peninsula. Abundant existing age data for the Zhaoyuan region deposits include Rb–Sr (Luo and Wu, 1987; Zhang et al., 1994), K–Ar (Lu and Kong, 1993; Sun et al., 1995), and $^{40}Ar/^{39}Ar$ measurements on alteration minerals (Li et al., 2003; X.O. Zhang et al., 2003; Li et al., 2006), Rb–Sr on fluid inclusion waters (Yang and Zhou, 2001), $^{40}Ar/^{39}Ar$ for quartz (Zhang et al., 2002), Rb–Sr on ore minerals (Zhang et al., 2002; Li et al., 2008), and U–Pb on a hydrothermal zircon (Hu et al., 2004). These data suggest the gold deposits in the Zhaoyuan area, and typically most elsewhere in the Jiaodong Peninsula, formed at ca. 120 ± 5 Ma. However, our recent geochronological work at the Dayingezhuang deposit, a large deposit located in the highly endowed northwestern part of the Jiaodong gold province, provides strong geochronological evidence for important gold deposition prior to 125 Ma in a distinct structural setting. This has led us to re-evaluate the duration of gold-forming event(s) and the associated implication for exploration in the province.

Prior to our work, existing absolute age data for the Dayingezhuang deposit were solely determined by whole rock K–Ar methods on auriferous sericitized granite and K-feldspar-altered granite, and both groups of analyses range imprecisely from 132 to 120 Ma (Xu, 1999). However, K–Ar ages can be influenced by argon loss, argon gain, inherited argon, and incomplete outgassing of polymerized felsic melts. These aspects of the K–Ar dating method can be partly explored by judicious choice of samples for measurement, but can be much more fully exploited using the $^{40}Ar/^{39}Ar$ dating technique to decipher the detailed thermal history of a given region (McDougall and Harrison, 1999), which led us to initially conduct this study. We have combined high-precision, step-heating $^{40}Ar/^{39}Ar$ geochronology on white micas with field observations to help resolve the chronology and duration of the ore-forming hydrothermal activity at the deposit. Combining these new data, with the existing geochronology for structural events, intrusive activity, and gold mineralization in the area, we discuss the timing of gold mineralization in the Dayingezhuang gold deposit and the duration of ore-forming hydrothermal activity during late Mesozoic in the Jiaodong gold province.

2. Regional geology

2.1. Terranes and lithologies

The eastern block of the North China Craton in Shandong Province is divided into two parts by the Tan–Lu (Tancheng–Lujiang) Fault, with the Jiaodong Peninsula to the east and the Luxi area to the west. The Jiaodong Peninsula is underlain by two Precambrian tectonic units, the Jiaobei terrane in the west and Sulu terrane in the east (Fig. 1). The Sulu terrane is the eastern end of the Dabie–Sulu ultrahigh-pressure metamorphic belt, which developed along the southern side of the North China Craton during ca. 240–220 Ma metamorphism of Proterozoic rocks (Hacker et al., 1998; Ayers et al., 2002). Paleoproterozoic amphibolite and granitic gneiss are exposed in the area of Haiyangsuo, which is located at the southernmost margin of the Sulu terrane (Li and Chen, 1994; Ye et al., 1999; Guo et al., 2002; Liou et al., 2006). In addition, ca. 800–700 Ma granitic gneiss is widely exposed in the Weihai, Rongcheng, and Wendeng areas (Ames et al., 1996; Wang and An, 1996).

The Jiaobei terrane, which hosts the vast majority of the gold deposits, consists of the Jiaobei uplift in the north and the Jiaolai basin in the south. Precambrian basement rocks exposed in the Jiaobei uplift are composed mainly of Neoarchean and younger tonalite–trondhjemite–granodiorite (TTG) gneisses (Jiaodong Group), and Paleoproterozoic (Fenzishan/Jinshan Group) and Neoproterozoic (Penglai Group) metasedimentary sequences (Lu, 1998; Wallis et al., 1999; Tang et al., 2007). The TTG gneisses are exposed in the center of the Jiaobei uplift. Protolith ages of the TTG gneisses are 2.9–1.9 Ga (Wang and An, 1996; Lu, 1998; Tang et al., 2007, 2008; Jahn et al., 2008), with metamorphic ages for the amphibolite- to granulite-facies rocks of ca.1.8–1.7 Ga (Zhai et al., 2000; Faure et al., 2003). The Jiaolai basin is a Cretaceous extensional basin, which is underlain by rocks of the middle Early Cretaceous Laiyang Group (sandy conglomerate and carbon-rich shale), late Early Cretaceous Qingshan Group (basalt, andesite, and trachyte tuff), and Late Cretaceous Wangshi Group (sandy conglomerate and siltstone; Lu and Dai, 1994; Ren et al., 2008).

2.2. Mesozoic granitoids

Mesozoic igneous rocks that intruded the Precambrian basement in Jiaodong cluster into four groups: Late Triassic syn-collisional granitoids, Late Jurassic calc-alkaline granitoids, Early Cretaceous high-K calc-alkaline granitoids, and late Early Cretaceous alkaline granitoids. The gold deposits are spatially associated with Late Jurassic and/or Early Cretaceous calc-alkaline granitoids, which are described in detail below.

Late Triassic syn-collisional granitoids, including the Shidao syenite–granitic complex (Chen et al., 2003; Yang et al., 2005), were emplaced into rocks of the Sulu terrane. The granitoids are mantle-derived (Song et al., 2003; Guo et al., 2005), and the syenitic bodies were emplaced at ~15 km depth (Zeng et al., 2007). These intrusions formed during the collision of North China and Yangtze Cratons at ca. 225–205 Ma (Chen et al., 2003; Guo et al., 2005).

Late Jurassic calc-alkaline granitoids are E–W trending across uplifted parts of both terranes. Most of the granites were intruded as components of a large batholith and include the Linglong, Kunyushan, Duogushan, and Wendeng bodies; the former two are widely deformed into gneissic rocks (Li and Yang, 1993). Compositions include biotite monzonitic granite, monzonitic diorite, quartz diorite, and granodiorite. However, there are different viewpoints as to whether the magmas are crustal melts (Hu et al., 1987; Wang et al., 1998), are derived from mantle sources (Chen et al., 1989), or are a type of hybrid system (Yao et al., 1990; Yang et al., 2013). These various opinions partly resulted from different views about the spatial relation between the granite and the Precambrian high-grade metamorphic rocks (Yang et al., 2007a). Application of high-precision dating, coupled with interpretation of detailed petrological and geochemical data, have led to a widely accepted understanding on the genesis of the Linglong granitoids in more recent years. These data indicate that the Linglong suite was derived by partial melting of Neoarchean lower-crustal rocks (Hou et al., 2007), with emplacement depths of 25–30 km (Zen and Hammarstrom, 1984; Chen et al., 1996). SHRIMP and LA–ICP-MS zircon U–Pb ages of the granitoids in the batholith are mainly between 160 and 150 Ma, although a few range from 147 to 142 Ma (Wang et al., 1998; Hu et al., 2004; Guo et al., 2005). Many Cretaceous felsic to mafic dikes, which have a broad range of reported ages (Wang et

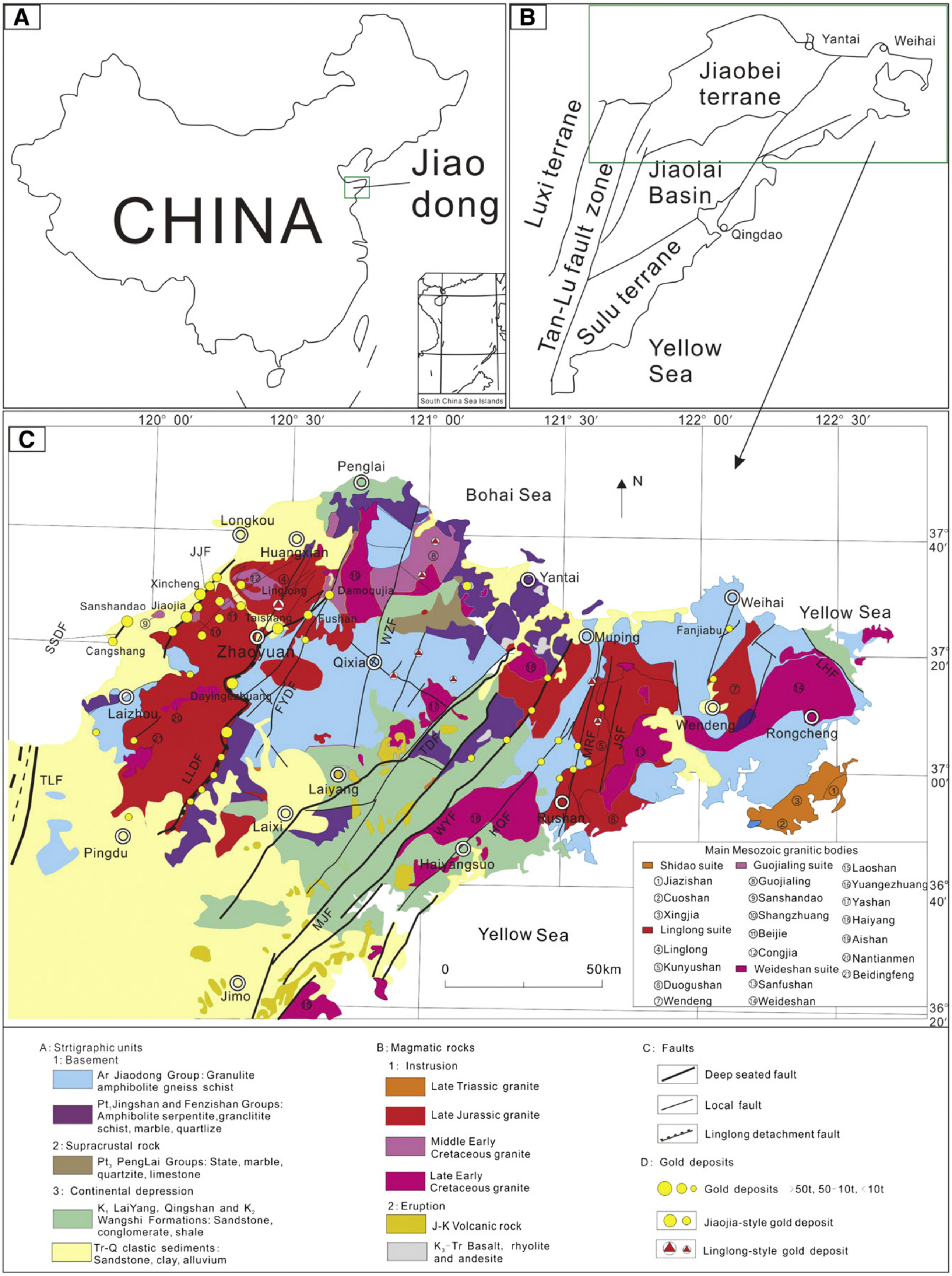

Fig. 1. Simplified geological map of the Jiaodong Peninsula showing location of the major gold deposits (modified from Deng et al., 2003; Chen et al., 2005; Yang et al., 2006). The Dayingezhuang gold deposit is located in the southeast part of the Jiaoxibei uplift, and along the part of the fault to the south of Zhaoyuan City, defined by Charles et al. (2011) as the Linglong detachment fault. Abbreviations: SSDF, Sanshandao Fault; JJF, Jiaojia Fault; ZPF, Zhaoping Fault; LLDF, Linglong detachment fault; FYDF, Fengyidian Fault; WZF, Wushilibao–Zixiantou Fault; TDF, Taocun–Dongdoushan Fault; MJF, Muping–Jimo Fault; WYF, Wulian–Yantai Fault; HQF, Haiyang–Qingdao Fault; MRF, Muping–Rushan Fault; JSF, Jiangjun–Shiquhe Fault; LHF, Lidao–Haixitou Fault.

al., 1998; Luo and Miao, 2002; Liu et al., 2004), cut these granitoids. The dikes, trending mainly NE and NNE, include lamprophyre, diorite, diorite porphyry, pegmatite, and syenite porphyry types.

Most workers now recognize many of the deeply emplaced syntectonic Jurassic bodies crystallized during compressional deformation and were uplifted during Early Cretaceous extension as parts of metamorphic core complexes (e.g., Davis et al., 1996, 2001). These massifs are characterized by deformed and mylonitized margins and massive cores (e.g., Qiu et al., 2002), with the margins defining relatively flat-lying, high-strain shear zones that are the sites of normal fault displacement. At Linglong within the Jurassic Jiaodong batholith, the intrusive rocks transitionally grade into highly deformed migmatitized granitoid along the eastern margin of the batholith; together the anatectic intrusions and migmatites form the lower part of the Late Jurassic Linglong Metamorphic Core Complex as is defined by Charles et al. (2011). They suggest a period of active detachment faulting occurred from at least 143 to 128 Ma (Charles et al., 2013).

Early Cretaceous high-K calc-alkaline granitoids are represented by the Guojialing-type porphyritic granodiorites in the northwestern corner of the Jiaodong Peninsula (Fig. 1). The Guojialing-type suite is composed of more than one dozen E–W-trending bodies with SHRIMP and LA–ICP-MS zircon U–Pb ages of 130–126 Ma (Hu et al., 1987; Wang et al., 1998; Yang and Zhou, 2001). These bodies, including Sanshandao, Shangzhuang, Beijie, Congjia, and Guojialing, show a compositional evolution from granite to granodiorite, and then to alkaline, from west to east in this uplifted part of the peninsula. Petrological and geochemical data indicate that the Guojialing-type suite was formed by the mixing of melt derived from delaminated eclogitic lower crust with upwelling asthenospheric mantle (Hou et al., 2007). The formation temperature, pressure, and emplacement depth of these synkinematic bodies is 655 °C ~ 764 °C, 200 ~ 350 MPa and 5–13 km, respectively, calculated from the Q–Ab–Or system phase diagram and from mineral geobarometry (Chen et al., 1993; Lin and Yin, 1998). Given the close spatial association with the gold deposits, many of which in the Zhaoyuan region are hosted by brittle faults on the margins of these plutons, pluton emplacement data also give a maximum estimate of depth of gold veining.

Late Early Cretaceous alkaline granitoids and high-K intermediate to mafic dikes are located in the Sulu UHP terrane and in the Jiaolai basin. These intrusions formed by crustal–mantle mixing when magma sources were changing from enriched mantle to depleted mantle due to lithospheric thinning (Yang et al., 2003). Zircon SHRIMP U–Pb ages of these rocks are ca. 125–90 Ma (Guo et al., 2005; Zhang and Zhang, 2007). The plutons of the Weideshan suite were emplaced into the northeastern edge of the Sulu terrane, at depths of ~30 km (Song et al., 2003).

3. Regional structure

Regional structures include E-, NE–NNE-, and NW–NNW-trending fault systems (Fig. 1). The gold mineralization is mainly controlled by the NE- to NNE-trending set of faults (Deng et al., 1996), as is described below.

The E-trending set of faults is the earliest of the Mesozoic structures. Their formation has been linked to the north–south compression associated with early Mesozoic collision between the North China and Yangtze cratons, and was synchronous with the formation of the Dabie–Sulu ultrahigh-pressure metamorphic rocks (Zhang et al., 2006). The E-trending faults are relatively poorly preserved throughout the region, but could have provided a basement control on the belt of east–west Jurassic plutons (Fig. 1). Furthermore, some workers have suggested a high density of gold deposits where the E-striking faults intersect the NE- to NNE-striking structures (e.g., Wang et al., 1984; Teng, 1985; Zhou, 1995; Deng et al., 2010).

The NE- to NNE-trending set of faults form the principal ore-controlling structures (Goldfarb et al., 2001; Qiu et al., 2002). They are argued to be subsidiary faults to the regional Tan–Lu Fault system, initially developed in eastern China as Late Jurassic sinistral faults that transect the Zhaoyuan area and as Early Cretaceous dextral faults that formed pull-part basins, such as the Jiaolai basin (Fig. 1; Xu et al., 1987; Y.Q. Zhang et al., 2003; Zhu et al., 2010). These faults are evenly distributed, at a spacing of about 35 km, and are parallel to each other across the peninsula. From west to east, these are defined as the Sanshandao, Jiaojia, Zhaoping, Qixia, Muping–Jimo, and Mouru faults (Fig. 1), which are associated with nearly 90% of the defined gold resource on the Jiaodong Peninsula (Lu and Kong, 1993; Qiu et al., 2002; Deng et al., 2006). Previous studies have shown that movements along all of these faults are long-lived, and that the Mesozoic deformation along these is complex and can be divided into four stages (Li and Yang, 1993; Deng et al., 2003). For example, the Muping–Jimo Fault experienced left-slip transpression during the Late Jurassic, extension or transtension during the Early Cretaceous gold event, transpression at the end of the Early Cretaceous, and right-slip transtension during the Late Cretaceous and Paleogene (Zhang et al., 2007).

The NW-trending set of faults, which are locally associated with late, minor silver mineralization (see below), developed during compressional events after the main gold mineralization. This is well recognized because they cut the NE- to NNE-trending set of faults (Deng et al., 1996, 2010). The Dayingezhuang Fault, which offsets the Dayingezhuang gold deposit (see below), is a prominent example of one of these NW-striking faults.

4. Dayingezhuang deposit geology

The Dayingezhuang gold deposit is located about 18 km southwest of Zhaoyuan City, in the southeastern part of the Jiaobei uplift, near the center of the Zhaoping Fault zone (Fig. 1). The pre-mining reserves were about 125 t Au at the end of 2011, including more than 35 t that had already been produced, with an estimated annual production slightly greater than 2.6 t Au. The deposit is a typical Jiaojia-style gold deposit (e.g., Qiu et al., 2002), and is therefore characterized by most high-grade orebodies being dominated by auriferous quartz–sulfide veinlets and stockworks. Wallrocks comprise both highly metamorphosed Precambrian sequences to the east and Mesozoic granitoid to the west. Precambrian sequences are composed of rocks of the Neoarchean Jiaodong Group and Paleoproterozoic Jingshan Group. Late Jurassic intrusions are composed of Linglong-type granites cut by numerous dikes of varied composition.

At the Dayingezhuang deposit, the gold mineralization is confined to the major NNE-trending Zhaoping Fault, which is cut by the post-ore NW-trending Dayingezhuang Fault (Fig. 2). The part of the Zhaoping Fault to the south of Zhaoyuan City, where it forms the eastern margin of the Linglong massif, has been termed the Linglong detachment fault (Fig. 1) by Charles et al. (2011). The Precambrian basement rocks form the hangingwall and the Linglong granitoids define the mineralized footwall of an uplifted dome that is recognized as a type of metamorphic core complex. Partial exhumation of the core complex took place at ca. 150–130 Ma (Charles et al., 2011), during a major period of Mesozoic extension along the eastern margin of China (e.g., Lin et al., 2008). Estimated maximum depths of gold deposition, as defined by above Guojialing-type pluton emplacement constraints, are 5–13 km within the Zhaoyuan area. This suggests that the Linglong granitoids were being uplifted at rates of at least 1 km/m.y. from emplacement depths of 25–30 km prior to the time of gold deposition because many of the ores are along the contact between the two groups of granitoids, as well as being hosted within or along the edges of the Linglong-type plutons.

The high-angle Dayingezhuang Fault zone cuts the main gold lode into two sections with 260–300 m of lateral offset (Figs. 2 and 3). The Dayingezhuang Fault is located at the southernmost area of widespread brittle deformation along the Linglong detachment fault, with cataclasites dominant locally on both sides of the Dayingezhuang Fault

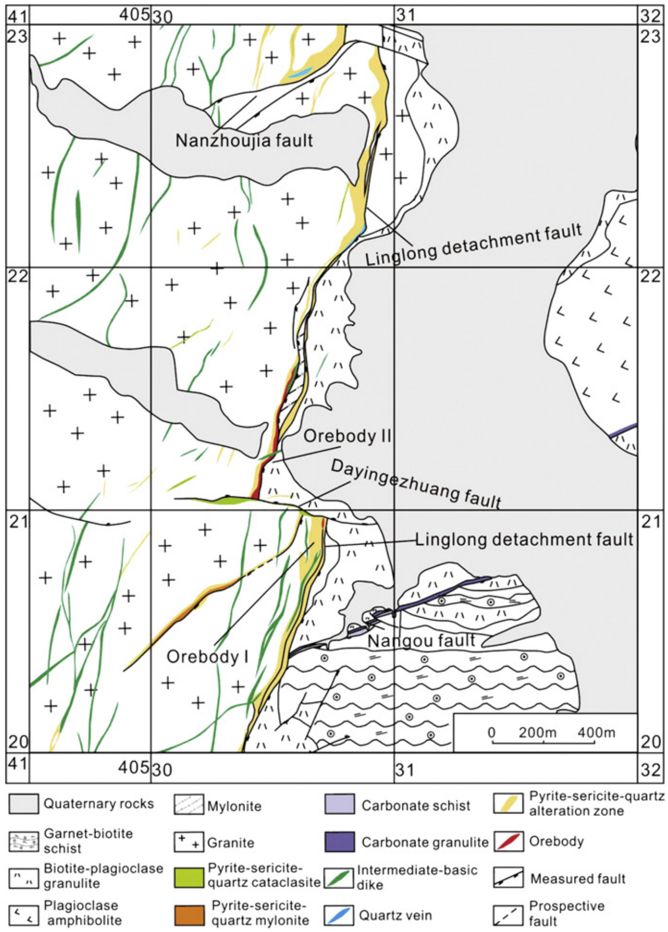

Fig. 2. General geological map of the Dayingezhuang gold deposit. Gold-bearing zones at the Dayingezhuang deposit are mainly controlled by the NE-trending Linglong detachment fault.

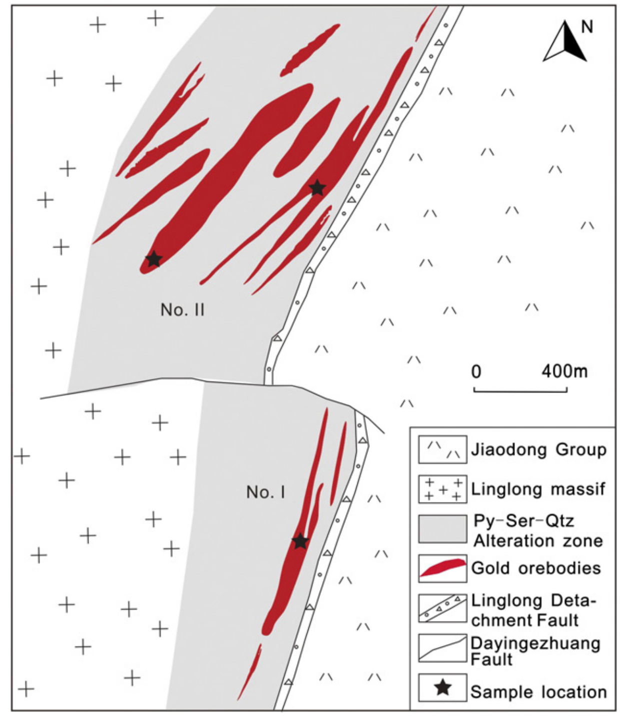

Fig. 3. Detailed geological map of orebodies in the Dayingezhuang gold deposit, showing the relationship between No. I and No. II orebodies and the location of samples collected for geochronology studies.

and also to the north, reflecting a late overprint to the ductile deformation. The earlier mylonitic features remain dominant at the granite's eastern margin along the length of the detachment to the south (Charles et al., 2011). The Dayingezhuang Fault may have developed post-ore because of the very different strain intensities (e.g., Charles et al., 2011) between the mylonitized rocks to the south and the brittle rocks to the north along the Linglong detachment fault. Alternatively, it may have originally been a pre-ore or syn-ore structure developed during the core complex exhumation.

Orebodies are hosted in quartz–sericite–pyrite altered and cataclastically deformed Linglong granite located in the footwall of the Linglong detachment fault zone, which dips to the southeast 21° to 58°. The variable dip is consistent with the well-accepted model of Spencer (1984) that indicates many low-angle "detachments" were originally moderately dipping normal faults and that some segments subsequently rotated to shallower angles during unloading of the footwall during doming. The barren hangingwall of the Linglong detachment fault is composed of rocks of the Precambrian Jiaodong Group. The NNE- to NE-trending Linglong detachment fault and the brecciated zones in the footwall control the occurrence of the orebodies (Fig. 2), with joints and fissures controlling local zones of high-grade gold mineralization (Zhai et al., 2002).

The No. I and II orebodies are the most important parts of the resource. They represent 85% of the proven reserves in the Dayingezhuang deposit, located south and north of the Dayingezhuang Fault, respectively (Fig. 3), and are described in detail below.

The No. I orebodies are composed of 18 ore lenses, including both continuous lodes and parallel ore zones, and they are mainly concentrated for about 60 m into the altered footwall rocks (Fig. 3). These individual orebodies are NE-trending (20°) and dip to the southeast from 27° to 40°, with an average length of 740 m and an average ore grade of 4.03 g/t Au. The thickness of these individual orebodies is mainly 2–10 m, with a maximum of 20 m (Fig. 3). Ores are dominated by pyrite–sericite–quartz altered rock (Fig. 4). Ore-bearing pyrite is mainly in veinlets cutting the cataclasite and disseminated in the intrusion, although some larger vein networks are present.

The No. I orebodies are different from the No. II orebodies based on higher silver grades and the presence of associated Pb- and Zn-bearing sulfides. The silver content in the ores gradually increases with depth, from 2 g/t at shallow (−140 m) to 50 g/t at the deeper levels (−380 m), with an average grade of 14.78 g/t; silver enrichment is associated with more abundant galena. Although silver grades are exceptionally high for gold orebodies in the Jiaodong province, silver is not of high enough grade to be recovered in the mining. There are no obvious reasons as to why the deeper parts of the No. I orebodies contain an abundance of silver-rich base metal sulfides.

The No. II orebodies are composed of 73 ore lenses, occurring as more irregular lodes and pods. They are mainly concentrated for about 60 m into the footwall and strike 20° (Fig. 3), and dip to the southeast from 28° to 53°, with an average length of 930 m and an average ore grade of 4.01 g/t Au. The thickness of these individual orebodies is mainly 10–30 m and the maximum width reaches 100 m. The orebodies are anastomosing and branching, and pinch-and-swell throughout most of their length (Fig. 3), suggesting ongoing high-strain ductile deformation. Because this is not observed in the No. I orebodies, this suggests the No. II orebodies are older. Ores are dominated by pyrite–sericite–quartz altered rock. Ore-bearing pyrite is mainly in veinlets and disseminated in the altered rocks (Fig. 4), and thus similar in style to that in the No. I orebodies.

Gold in the No. I and No. II orebodies is present as silver-bearing native gold and electrum. It occurs as free gold (75%), gold in fissures in sulfides (20%), and gold inclusions in sulfides (5%), and is most closely associated with pyrite, and lesser chalcopyrite, galena, and sphalerite (Fig. 4E and F). Identified silver-bearing minerals in the

No. I orebodies include native silver, küstelite, hessite, argentite, acanthite, polybasite, and pearceite, with lesser freibergite and argentobismutite. These are mainly hosted in quartz, with rare inclusions in sulfides (Fig. 4G). Microscopic studies show gold-bearing phases were deposited before the silver minerals. The presence of a large number of silver minerals in the No. I orebodies of the Dayingezhuang gold deposit makes this deposit unique from other Jiaodong deposits. Other sulfides in the deposit include pyrrhotite and bismuthinite.

The bulk of the ore is within and surrounded by zones of strong silicification, sericitization, sulfidation, and K-feldspar alteration; the K-feldspar and sericite extend beyond the limits of the pyrite and silicification. Although the ore fluids were CO_2-rich (Yang et al., 2009), the very limited carbonate alteration and typically

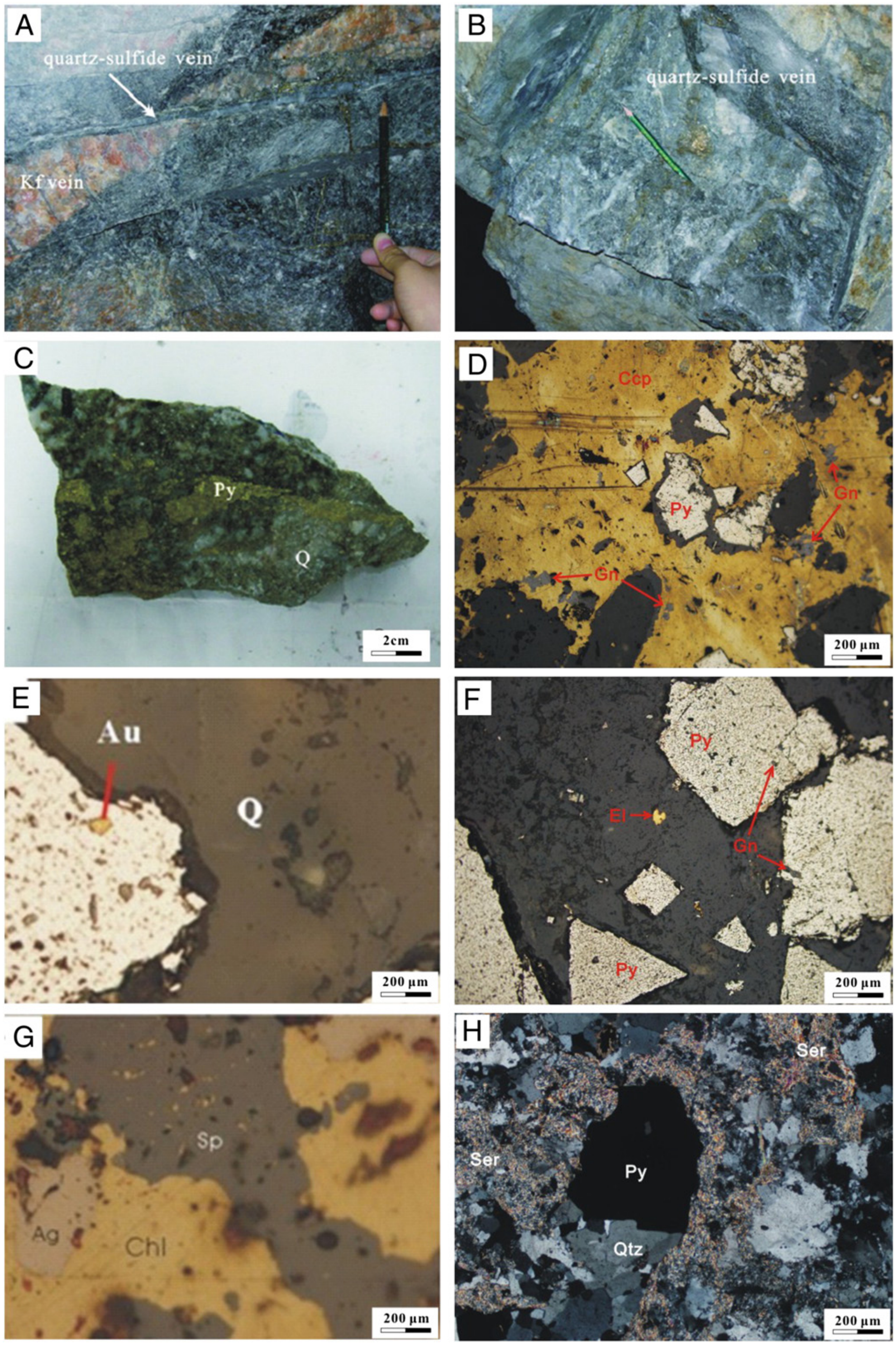

Fig. 4. Photograph of the ore type and microphotograph and SEM images of the minerals and texture. A. Quartz–sulfide vein cutting a K-feldspar-rich vein (Line 61, Level −290 m). B. Quartz–sulfide vein in No. I ore body (Line 61, Level 250 m, where y61250k was sampled). C. Vein type mineralization ore specimen (y725245k). D. Chalcopyrite, pyrite, and galena (y725245k). E. Gold inclusion (y61250k). F. Intercrystalline gold (y61250k). G. Silver inclusion. H and I. Sericite selected for $^{40}Ar/^{39}Ar$ dating, transmitted light (+) (y61250k and y725245k). J and K and L. Sericite and muscovite selected for $^{40}Ar/^{39}Ar$ dating, transmitted light (+) (y745380kI and y745380kII). M and N. Scanning electron microscope (SEM) image of sericite selected for $^{40}Ar/^{39}Ar$ dating (y61250k). O and P. SEM image of muscovite selected for $^{40}Ar/^{39}Ar$ dating (y745380kI and y745380kII).

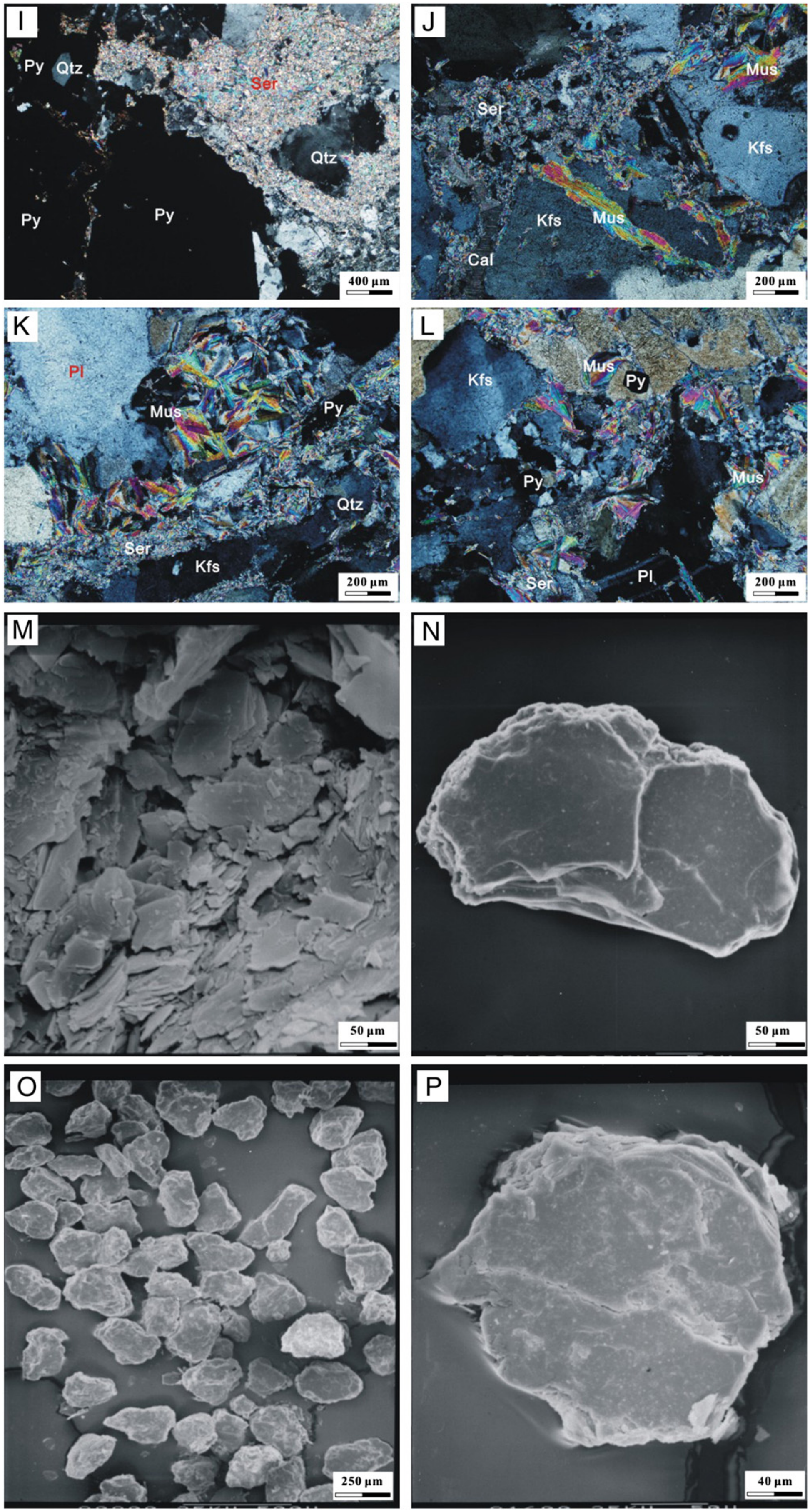

Fig. 4 (*continued*).

massive pyrite are consistent with a fluid in equilibrium with a high Fe/(Fe + Mg) rock, as is common with many granitoids (e.g., Bohlke, 1988). The Precambrian metamorphic rocks in the hangingwall of the Linglong detachment fault zone are only very weakly altered, and are characterized by carbonatization and chloritization, weak silicification, and slightly anomalous gold (<0.1 ppm).

5. Geochronology of gold mineralization

5.1. Sample collection

To investigate the timing of gold mineralization, and resulting implications for both ore genesis and for late Mesozoic tectonic evolution, three sericite and one muscovite samples for $^{40}Ar/^{39}Ar$ geochronology were collected from three widely spaced locations in orebodies I and II (Fig. 3). These sites are described below.

Sample y61250k was collected from the center of the No. I orebodies at the −250 m level (Fig. 3), in an area dominated by quartz–sulfide veinlets (Fig. 4B). The altered granite is gray-white in color, generally massive, and with a granoblastic texture (Fig. 4H). The rock is composed of quartz (about 45%), sericite (about 25%), plagioclase (about 5%), K-feldspar (about 10%), pyrite (about 10%), and traces of chalcopyrite, galena, gold, and electrum (Fig. 4E and F). Sericite grains are about 0.01–0.2 mm in length, formed from the hydrothermal alteration of feldspar, are closely associated with the euhedral and subhedral pyrite (Fig. 4H), and show almost colorless to very pale green polychroism and the same interference color of Level 3. Scanning electron microscope (SEM) images show the sericite occurs as subhedral hexagonal plates or anhedral grains (Fig. 4M and N).

Sample y725245k from the No. II orebodies was collected from a zone of gold mineralization at the −245 m level (Fig. 3), dominated by chalcopyrite veinlets and disseminated pyrite (Fig. 4C). All features of the sampled zone (Fig. 4I) and collected sericite are identical to those of sample y61250k, although the massive granite here consists of quartz (about 35%), sericite (about 35%), plagioclase (about 5%), K-feldspar (about 8%), and chalcopyrite, pyrrhotite, and pyrite (about 15%), with traces of galena and bismuthinite (Fig. 4D). In addition, the sericite is closely associated with the anhedral chalcopyrite and pyrite (Fig. 4I), and is present as subhedral hexagonal plates or anhedral grains (Fig. 4M and N).

At a third site, both hydrothermal sericite and coarser muscovite were visible in the ores. Sample y745380kI and Sample y745380kII from the No. II orebodies were collected from the same site in a zone of gold mineralization at the −400 m level (Fig. 3). The zone contains quartz (about 50%), sericite (about 15%), muscovite (about 10%), plagioclase (about 10%), K-feldspar (about 10%), pyrite and chalcopyrite (about 5%), and minor calcite (Fig. 4J). The sericite is the same size as that from the other two locations and is closely associated with the euhedral and subhedral pyrite (Fig. 4K). Muscovite in the sample shows similar interference colors and polychroism, but is distinguished because it is distinctly larger (about 0.05–0.5 mm) and has brighter interference colors than the sericite (Fig. 4J). Nevertheless, both phases of white mica were formed from the hydrothermal alteration of feldspar and are associated with the euhedral and subhedral pyrite (Fig. 4L). The SEM images show that both the sericite and muscovite (Fig. 4O and P) occur as subhedral hexagonal plates or anhedral grains.

5.2. Experimental method

Muscovite and sericite grains were crushed and sieved to 125 to 250 μm and separated from the other phases in the altered granites by conventional heavy-liquid, magnetic, and hand separation techniques to achieve >99% purity at the Langfang Regional Geological Survey, Hebei Province, China. The mineral separate, Fish Canyon Tuff sanidine and ZBH-25 biotite (standard sample in China) flux monitors were irradiated in the atomic reactor of Research Institute of Atomic Energy (Beijing, China) and set in the H8 hole for fast neutron irradiation. The irradiation duration and neutron dose were 10.7 h and 2.45×10^{17} n/cm^2 for the analyzed minerals, respectively. The J factor was estimated by replicate analysis of Fish Canyon Tuff sanidine, with an age of 27.55 ± 0.08 Ma (Lanphere and Baadsgaard, 1997), and the ZBH-25 biotite standard with an age of 133.3 ± 0.24 Ma (Fu et al., 1987) with 1% relative standard deviation (1σ). The J-values for individual samples were determined by a second-order polynomial interpolation. The Ca and K correction factors were calculated from co-irradiation of pure salts of CaF_2 and K_2SO_4 [e.g., $(^{40}Ar/^{39}Ar)_K = 0.004782$, $(^{39}Ar/^{37}Ar)_{Ca} = 0.00081$, $(^{36}Ar/^{37}Ar)_{Ca} = 0.0002398$].

The $^{40}Ar/^{39}Ar$ analyses were performed at the Geologic Laboratories Center, China University of Geosciences, Beijing, on a MM5400 Micromass spectrometer operating in a static mode. Samples were loaded in aluminum packets into a Christmas tree sample holder and degassed at low temperature (250–300 °C) for 20–30 min before being incrementally heated in a double-vacuum furnace. The gases released during each step were purified by means of Ti and Al–Zr getters. Once cleaned, the gas was introduced into a MM-5400 Micromass spectrometer, and 4–5 min were allowed for equilibration before static analysis was done.

The ^{40}Ar, ^{39}Ar, ^{38}Ar, ^{37}Ar, and ^{36}Ar isotopic abundances were determined through linear extrapolation at time zero of peak intensities. The data were corrected for system blanks, mass discriminations, interfering Ca, K-derived argon isotopes, and the decay of ^{37}Ar since the time of the irradiation. The decay constant used throughout the calculations is $\lambda = (5.543 \pm 0.010) \times 10^{-10}$ a^{-1}. Dates and errors were calculated using a computer program from the Berkeley Geochronological Center. All errors are reported as 1σ.

The $^{40}Ar/^{39}Ar$ data are listed in Table 1, and released spectra are shown in Fig. 6. Weighted mean plateau ages are reported where >50% of the released ^{39}Ar in contiguous steps is within 1σ error. The closure temperature of argon diffusion of muscovite has been generally assumed to be about 400 ± 50 °C for a relatively rapid cooling rate, 360 °C to 350 °C for a moderate cooling rate (Hames and Bowring, 1994; McDougall and Harrison, 1999), and 270 °C during slow cooling or extended reheating (Snee et al., 1988). More recently, Harrison et al. (2009) suggested muscovite closure temperatures in excess of 400 °C for slow cooling.

5.3. $^{40}Ar/^{39}Ar$ results

The three sericite samples and one muscovite yield well-defined $^{40}Ar/^{39}Ar$ plateau ages. The $^{40}Ar/^{39}Ar$ plateau ages of muscovite (y745380kII) and sericite (y745380kI, y725245k) from the No. II orebodies, and sericite (y61250k) from the No. I orebodies, within error at the one sigma level and calculated from about 93.5 to 98.4% of the released ^{39}Ar, are 128.67 ± 0.50 Ma, 130.52 ± 0.52 Ma, 133.37 ± 0.56 Ma, and 126.8 ± 0.59 Ma (Fig. 5), respectively. The isochron ages are similar to the plateau ages, agreeing within error (Fig. 5).

In order to discuss the difference among the age data for these four samples, we have recalculated the $^{40}Ar/^{39}Ar$ plateau ages to include the error in the J-value. The $^{40}Ar/^{39}Ar$ plateau ages of muscovite (y745380kII), sericite (y745380kI), and sericite (y725245k), within error at the two sigma level and calculated from about 91.5, 96.4, and 81.3% of the released ^{39}Ar, are 128.38 ± 0.69 Ma, 130.71 ± 0.70 Ma, and 132.74 ± 0.83 Ma (Fig. 6), respectively, showing they are statistically indistinguishable. Because we were unable to collect >50% of the released ^{39}Ar in contiguous steps within 2σ error in the age spectra of sericite (y61250k), the $^{40}Ar/^{39}Ar$ plateau age within error at the two sigma level could not be obtained.

Table 1
$^{40}Ar/^{39}Ar$ step-heating geochronology data for sericite and muscovite from Dayingezhuang gold deposit in Jiaodong gold province.

Temp (°C)	$(^{40}Ar/^{39}Ar)m$	$(^{36}Ar/^{39}Ar)m$	$(^{37}Ar/^{39}Ar)m$	$(^{40}Ar^{a}/^{39}Ar_{k})m$	^{39}Ar (E12 mol)	^{39}Ar (%)	$^{40}Ar^{a}$ (%)	Age (Ma)	Error (1σ, Ma)
Sample number = y745380kI; mineral = sericite; wt. = 0.04447 g; J = 0.002167.									
730	57.899	0.107	0.074	26.224	0.076	0.45	46	99.71	4.51
830	39.227	0.018	0.002	33.863	0.334	1.97	86.5	127.75	2.02
880	38.204	0.011	0.019	34.988	0.414	2.45	91.69	131.84	1.87
920	46.976	0.042	0.008	34.552	0.247	1.46	73.9	130.25	2.28
960	39.395	0.016	0.005	34.719	1.057	6.25	88.28	130.86	2.05
1000	36.53	0.006	0.007	34.657	0.77	4.55	94.94	130.64	1.94
1040	36.002	0.005	0.008	34.409	1.476	8.72	95.63	129.74	2.71
1080	35.649	0.004	0.004	34.526	1.569	9.28	96.89	130.16	2.59
1120	36.353	0.004	0.006	35.252	1.681	9.93	97.01	132.8	5.46
1160	35.706	0.004	0.001	34.593	2.207	13.04	96.92	130.4	1.78
1200	35.908	0.004	0.005	34.574	2.855	16.87	96.33	130.34	1.26
1240	35.745	0.004	0.003	34.687	2.589	15.3	97.08	130.75	1.26
1340	36.649	0.006	0.018	34.773	1.449	8.56	94.95	131.06	1.29
1400	48.101	0.026	0.059	40.456	0.196	1.16	84.31	151.6	2.3
Sample number = y745380kII; mineral = muscovite; wt. = 0.03731 g; J = 0.002163.									
710	52.066	0.076	0.113	29.488	0.072	0.47	57.20	111.54	4.51
820	38.833	0.026	0.056	31.232	0.182	1.17	80.68	117.93	2.54
880	36.100	0.000	0.015	36.030	0.294	1.89	99.81	135.38	1.88
920	47.220	0.044	0.018	34.083	0.534	3.43	72.54	128.32	1.86
960	38.798	0.016	0.006	34.201	0.709	4.55	88.31	128.75	1.79
1000	35.779	0.006	0.006	34.057	1.015	6.52	95.25	128.22	1.78
1040	35.738	0.006	0.004	34.074	0.930	5.98	95.40	128.29	1.79
1080	35.193	0.004	0.006	34.023	1.965	12.63	96.72	128.10	1.76
1120	35.119	0.004	0.007	34.035	1.607	10.33	96.95	128.15	1.81
1160	35.128	0.004	0.004	34.034	2.264	14.55	96.92	128.14	1.76
1200	35.426	0.004	0.003	34.165	2.144	13.77	96.49	128.62	1.29
1280	35.411	0.004	0.003	34.140	3.071	19.73	96.46	128.53	1.25
1340	38.135	0.012	0.006	34.691	0.628	4.03	91.09	130.53	1.37
1400	47.939	0.033	0.072	38.304	0.148	0.95	80.16	143.59	2.64
Sample number = y725245k; mineral = sericite; wt. = 0.05005 g; J = 0.002169.									
700	50.529	0.078	0.031	27.389	0.070	0.35	54.80	104.11	5.24
820	40.568	0.016	0.008	35.737	0.332	1.68	88.25	134.68	2.06
880	37.964	0.008	0.002	35.587	0.610	3.07	93.82	134.13	1.95
920	37.964	0.000	0.021	37.925	0.273	1.37	99.90	142.61	2.04
960	41.463	0.020	0.003	35.522	1.449	7.30	85.86	133.90	1.84
1000	36.841	0.000	0.007	36.812	0.986	4.97	99.92	138.58	1.89
1040	36.588	0.004	0.010	35.283	1.614	8.13	96.48	133.03	1.82
1080	36.564	0.004	0.002	35.253	2.063	10.39	96.46	132.92	1.82
1120	36.676	0.005	0.004	35.143	1.697	8.55	95.87	132.52	1.82
1160	36.743	0.006	0.001	35.020	2.153	10.85	95.37	132.07	1.80
1200	37.138	0.007	0.011	35.152	2.428	12.24	94.72	132.56	1.28
1260	37.063	0.006	0.005	35.420	3.747	18.88	95.63	133.53	2.53
1400	37.074	0.006	0.006	35.260	2.422	12.21	95.17	132.95	1.29
Sample number = y61250k; mineral = sericite; wt. = 0.06001; J = 0.002165.									
700	56.025	0.114	0.006	22.318	0.085	0.27	40.62	85.12	2.80
780	53.825	0.003	0.033	53.015	0.027	0.09	98.51	196.01	6.21
860	35.563	0.011	0.018	32.346	0.414	1.32	91.07	122.11	1.74
920	40.190	0.023	0.005	33.263	0.939	3.00	82.99	125.45	1.73
960	36.018	0.008	0.001	33.736	0.797	2.54	93.75	127.17	1.78
1000	34.655	0.003	0.004	33.772	2.158	6.88	97.49	127.30	1.74
1040	34.944	0.004	0.004	33.864	1.736	5.54	96.95	127.64	1.75
1080	34.564	0.003	0.006	33.806	2.074	6.61	97.83	127.43	1.75
1120	34.355	0.002	0.006	33.755	2.481	7.91	98.28	127.24	1.74
1160	32.993	0.001	0.005	32.557	4.288	13.68	98.69	122.87	1.85
1200	34.677	0.003	0.006	33.927	10.385	33.12	97.86	127.87	1.24
1250	34.628	0.000	0.005	34.617	3.213	10.25	99.97	130.37	1.33
1300	35.509	0.000	0.010	35.480	1.627	5.19	99.92	133.51	1.30
1350	40.824	0.014	0.006	36.824	0.463	1.48	90.33	138.38	1.48
1400	56.5612	0.031634	0.06167	47.2153	0.670	2.14	83.69	175.58	2.44

Note: Time of each step-heating is 10 min.
[a] Radiogenic.

6. Discussion

6.1. Timing of gold mineralization at the Dayingezhuang gold deposit

Well-defined plateau ages of four mica samples indicate that they are reliable estimates of the timing of hydrothermal alteration. The minimum temperature of gold deposition in the investigated deposit, estimated from homogenization temperature of fluid inclusions in auriferous quartz, ranges from 240 °C to 360 °C (Yang et al., 2009), although trapping temperature of the ore fluids could be slightly higher if pressure corrections were required. Coexistence of ductile deformation of the quartz associated with pyrite (Fig. 4H and I) and brittle

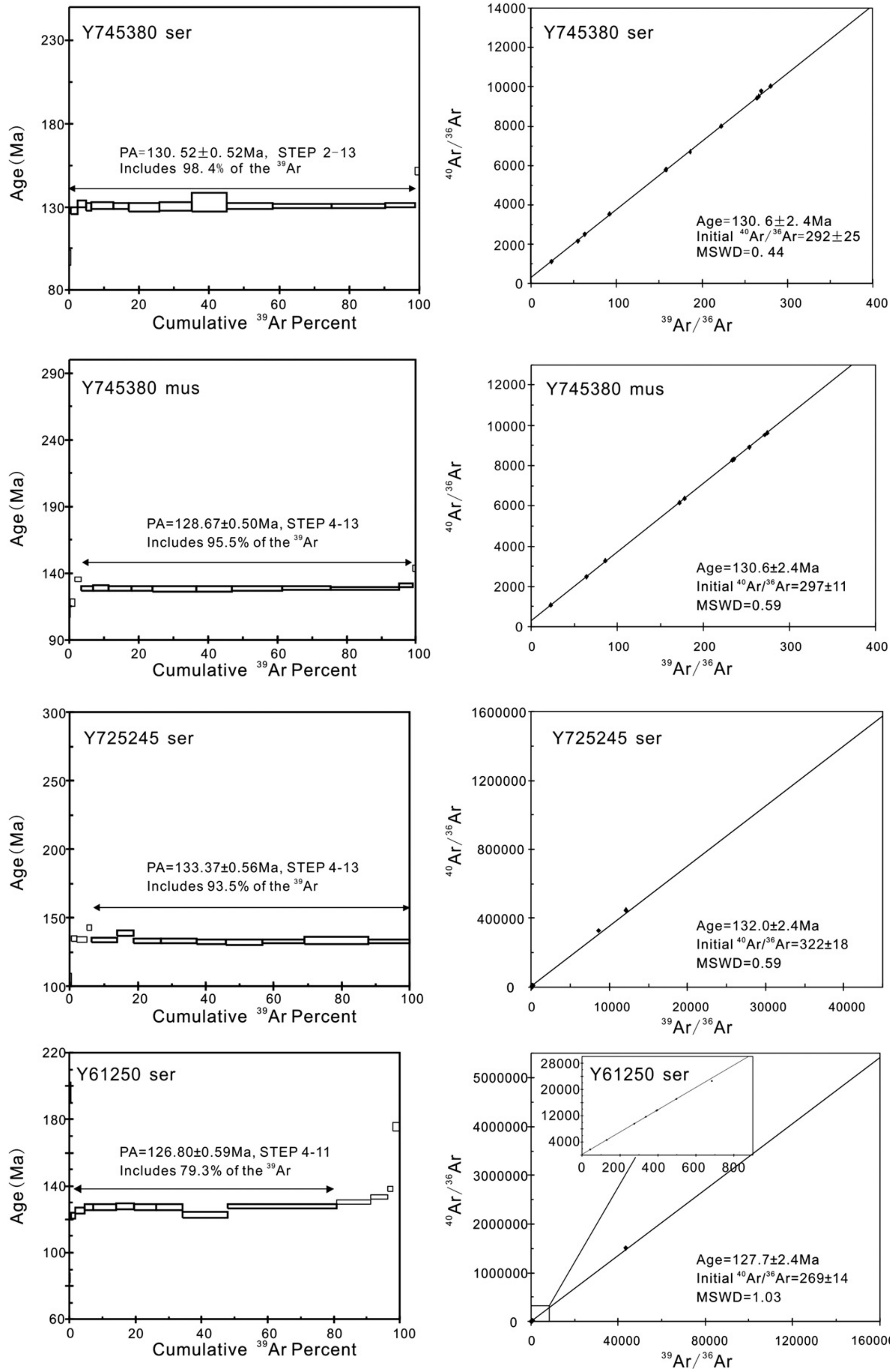

Fig. 5. $^{40}Ar/^{39}Ar$ plateau and isochron ages (1σ) for sericite and muscovite from the Dayingezhuang gold deposit. The following abbreviations are used: Ser, sericite; Mus, muscovite; PA, preferred age.

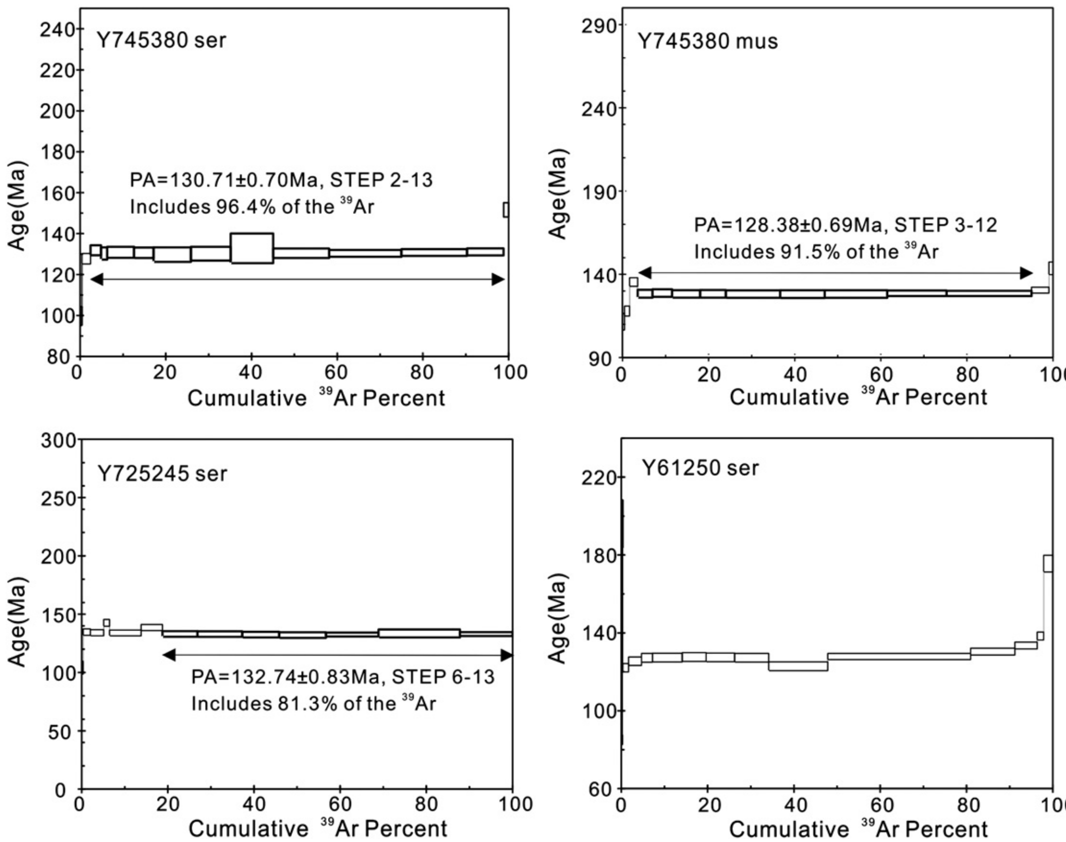

Fig. 6. $^{40}Ar/^{39}Ar$ plateau ages (2σ) for sericite and muscovite from the Dayingezhuang gold deposit. The following abbreviations are used: Ser, sericite; Mus, muscovite; PA, preferred age.

deformation of sericitized feldspar (Fig. 4J) in the ores at the Dayingezhuang gold deposit could also indicate that deformation, and thus gold deposition, occurred under temperature conditions of ~300–400 °C (e.g., Passchier and Trouw, 2005). This relationship would hold true if the secondary feldspar was coeval with the main mineralization; a consistent spatial association between the orebodies and large clots of the feldspar in surrounding wallrock suggest this is a likely scenario. Given that the location of the deposit along the Linglong detachment fault zone is at the boundary between brittle and ductile deformation of the footwall granitoids (e.g., Charles et al., 2011), and such a transition is commonly observed in the 300–450 °C temperature interval in the upper crust, the above ore-forming temperature estimate of 300–400 °C seems very realistic.

The previously stated muscovite blocking temperatures, coupled with the above estimated ore formation temperatures, indicate that the ages of the argon plateaus represent the approximate mineralization age, irrespective of whether the hydrothermally altered rocks were undergoing slow or rapid cooling subsequent to the gold event. The weighted mean plateau $^{40}Ar/^{39}Ar$ data (2σ) from the Dayingezhuang deposit are indistinguishable from each other, and the weighted mean plateau $^{40}Ar/^{39}Ar$ data (1σ) range from 126.8 ± 0.59 Ma to 133.37 ± 0.56 Ma, indicating that they were formed contemporaneously in the middle Early Cretaceous (Figs. 5 and 6).

Thus, our study provides the first precise age data on the Dayingezhuang gold mineralization. More significantly, it unequivocally extends the oldest bound of the period of hydrothermal activity in the gold province to between 126.8 ± 0.59 Ma and 133.37 ± 0.56 Ma.

In contrast to the Dayingezhuang gold deposit, many of the other large gold deposits in the northwestern part of Jiaodong gold province, such as Cangshang, Jiaojia, Xincheng and Wang'ershan, located adjacent to the NE- to NNE-trending shear zones on the margins of Guojialing granite, formed between 125 and 115 Ma (Li et al., 2003; X.O. Zhang et al., 2003; Y.Q. Zhang et al., 2003) when using the most precise geochronology in the literature. The muscovite $^{40}Ar/^{39}Ar$ plateau age within error at the two sigma of Cangshang is 121.3 ± 0.2 Ma (X.O. Zhang et al., 2003). The sericite $^{40}Ar/^{39}Ar$ plateau ages within error at the two sigma of Jiaojia, Xincheng and Wang'ershan are 120.5 ± 0.6 Ma, 120.9 ± 0.3 Ma, and 119.8 ± 0.2 Ma, (Li et al., 2003), respectively.

6.2. Comparison with previous geochronological data

Existing K–Ar data for the Dayingezhuang deposit overlap our relatively narrow range of new ages, but are less precise. The whole-rock K–Ar dates of K-feldspar-altered granite and sericite-altered granite are both 126 ± 6 Ma (Xu, 1999). The poorer precision of the K–Ar dating left a great deal of uncertainty in defining the absolute age, particularly as to whether some gold in Jiaodong may have been older than previously determined for most of the other deposits.

The whole-rock K–Ar age for the unaltered Linglong granite at the Dayingezhuang deposit is 144 ± 7 Ma (Table 2; Xu, 1999), which, within error, overlaps the younger part of the ca. 160–150 Ma U–Pb crystallization age of the majority of the Linglong granites (Wang et al., 1998; Hu et al., 2004; Guo et al., 2005). Furthermore, K–Ar dates on granites often underestimate the age of the granites due to incomplete degassing of polymerized melts and argon loss effects. So there is little doubt that the gold ores are 20–30 m.y. younger than their immediate igneous host rocks. Based on cross-cutting relationships, pre-mineralization pegmatites (Fig. 4A) at the Dayingezhuang deposit yielded a whole-rock K–Ar date of 129 ± 6 Ma (Xu, 1999), and this indicates that the gold has a maximum age of 135 Ma. Similarly, the whole-rock K–Ar age for post-mineralization diorite porphyry dike

Table 2
Summary of direct $^{40}Ar/^{39}Ar$ and indirect K–Ar ages constrains on gold mineralization of Dayingezhuang gold deposit in Jiaodong gold province.

Sample	Rock name	Mineral	Method	Age (Ma)	References
Y745380KI	Pyrite–sericite–quartz gold ore	Sericite	Ar–Ar	130.52 ± 0.52 (P)	This paper
Y745380KII	Pyrite–sericite–quartz gold ore	Muscovite	Ar–Ar	128.67 ± 0.50 (P)	This paper
Y725245K	Pyrite–sericite–quartz gold ore	Sericite	Ar–Ar	133.37 ± 0.56 (P)	This paper
Y61250K	Pyrite–sericite–quartz silver-polymetallic ore	Sericite	Ar–Ar	126.8 ± 0.59 (P)	This paper
9880304	Fresh unaltered granite	Whole rock	K–Ar	144 ± 7	Xu (1999)
9880302	Pegmatite vein	Whole rock	K–Ar	129 ± 6	Xu (1999)
9880303	K-feldspar altered granite	Whole rock	K–Ar	126 ± 6	Xu (1999)
9692611	Sericite quartzite altered granite	Whole rock	K–Ar	126 ± 6	Xu (1999)
88-j-6	Fault gouge of Zhaoping Fault	Chlorite	K–Ar	136.86 ± 8.35	Deng et al. (1996)
	Post-mineralization K-feldspar altered granite vein	Whole rock	K–Ar	114.18 ± 16.7	Guo et al. (1990)
	Post-mineralization diorite porphyrite intruding the Zhaoping Fault and orebody	Whole rock	K–Ar	129.25 ± 2.25	Guo et al. (1990)

emplacement along the Zhaoping Fault zone is 129 ± 2 Ma (Guo et al., 1990), which places a minimum age constraint of 127 Ma on the gold event. Thus, although less precise, the existing K–Ar constraints bracket the time of mineralization to a relatively older time period than the other reliable ages for the mineralization in the Zhaoyuan region. Again, if the K–Ar dates are minimum age estimates, ore formation would be even older. Our new $^{40}Ar/^{39}Ar$ ages, however, more precisely confirm that the gold mineralization at Dayingezhuang occurred between 134 and 126 Ma (Fig. 7), which is a period nevertheless nearly identical to that suggested by the less dependable K–Ar studies of the pre- and post-ore dikes.

6.3. Duration of ore-forming hydrothermal activity

Our study of the $^{40}Ar/^{39}Ar$ systematics of the mineralization of the Dayingezhuang deposit shows that the main phase of gold mineralization there is constrained to the period 130 ± 4 Ma, which is older than 120 ± 5 Ma, the widely accepted main ore-forming period of the other major gold deposits in the northwestern part of the Jiaodong gold province (Yang et al., 2000; Yang and Zhou, 2001; Li et al., 2003; X.O. Zhang et al., 2003; Li et al., 2006, 2008; Guo et al., 2013; Yang et al., 2013). Some workers have broadly indicated that the gold event in the Zhaoyuan area was ca. 130–110 Ma (e.g., Qiu et al., 2002; Chen et al., 2005), but evaluation of only the most reliable geochronology among the existing data, as described above, has led to the general conclusion of a 120 ± 5 Ma gold event. However, our new data now suggest a significant older gold pulse did occur in the Zhaoyuan area. Although it is still uncertain as to whether gold formation is best defined as one continuous and evolving event or multiple and distinct episodes of a gold-forming period, when we consider the most precise dates from other workers and our new dates, the duration of ore formation in this giant gold province was at least 15–20 million years.

The duration of this older gold pulse itself is difficult to define. The fact that our youngest new date of 126.8 Ma characterizes the No. I

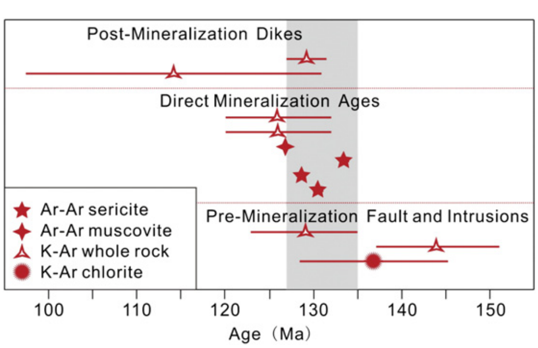

Fig. 7. Diagram indicating the ages determined for minerals and whole rocks from Dayingezhuang deposit. The 1σ analytical uncertainties are indicated by a solid line. The shaded interval indicates the ca. 130 ± 4 Ma period of gold mineralization in the Dayingezhuang gold deposit.

orebodies hints at an evolution to the more Ag–Pb–Zn-rich gold ore during the latter stages of the hydrothermal pulse. This is supported by the fact that the pinch-and-swell nature of the ores is restricted to the more northerly No. II orebodies, whereas no such strain seems to have impacted the No. I orebodies. In addition, we interpret the four dates, with well-defined plateaus and small errors, as a whole to indicate fluid movement and gold deposition during reactivation of the Linglong detachment fault occurred over as period of at least six to eight million years.

Charles et al. (2013) indicate that ductile deformation along the Linglong detachment fault continued until at least ca. 135.5–132.5 Ma and brittle overprinting was ongoing between ca. 129.5 Ma and 126.3 Ma. These data are consistent with our new deposit data that indicate gold was deposited during brittle deformation at this time and the oldest gold may have been deposited towards the end of the older ductile event. Many smaller gold deposits occur along the detachment further to the south (Fig. 1), but the transition to a more brittle regime may have been critical for localization of large orebodies, such as at the Dayingezhuang gold deposit.

6.4. Tectonic significance of new age data

The Dayingezhuang gold deposit is the only significant gold deposit (>100 t Au) along the Linglong detachment fault. Other undated deposits to the south along the structure are smaller and within areas of ductile deformation within the footwall to the fault. The larger Dayingezhuang deposit suggests a major hydrothermal event near the section of the fault zone that was characterized by a brittle–ductile transition at ca. 130 Ma. The association of gold with the cataclasites indicates brittle deformation and ore formation along the margin of the rapidly uplifting Linglong massif as it passed through a depth somewhere between 5 and 13 km. The hydrothermal activity is clearly responsible for brittle deformation and the resulting brecciation (e.g., see fig. 4H of Charles et al., 2011). Brecciated rocks along the detachment for about 20 km to the north may define other targets for large ca. 130 Ma gold deposits.

In contrast to the Dayingezhuang gold deposit, many of the other large gold deposits, such as Taishang and Damoqujia (Yang et al., 2007b, 2008), in the Zhaoyuan area are located adjacent to the NE- to NNE-trending faults along the margins of the Guojialing plutons that intruded the Linglong massif at 130–126 Ma. An $^{40}Ar/^{39}Ar$ date on biotite from the Guojialing pluton of 124 Ma (Charles et al., 2011) indicates very rapid uplift was ongoing immediately after crystallization of the Guojialing suite of plutons and during widespread gold formation. The brittle reactivation of these faults at ca. 120 ± 5 Ma, during the uplift, represents a subsequent episode of mineralization that is temporally distinct from that along the Linglong detachment fault. It may reflect successive periods of ductile to brittle transition along the uplifting margins of first the southeastern side of the Linglong massif and secondly the younger intrusions. Such mylonitization followed by cataclastic reactivation, as is characteristic

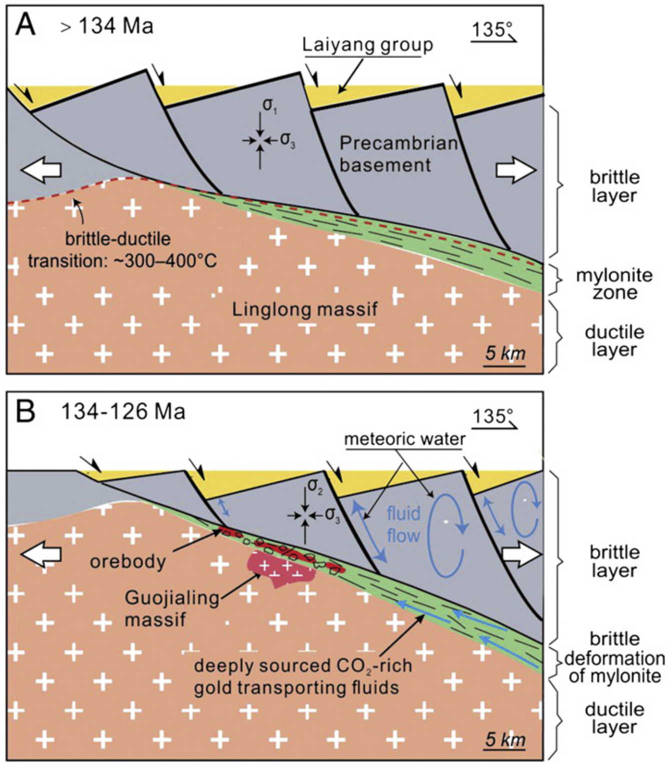

Fig. 8. Suggested model showing stages for core complex formation and gold mineralization. A. The ductile deformation under the NW–SE extension before ca. 134 Ma. B. The later brittle overprint and gold deposition at ca. 134–126 Ma.

of the Linglong detachment fault and the NE- and NNE-trending faults, typically characterizes the evolution of many core complexes (e.g., Davis and Lister, 1988).

The North China Craton represents an atypical example where lode gold deposits are hosted in terranes that are billions of years older than ore formation. The gold event on the Jiaodong Peninsula may ultimately relate to major plate shifts in the Pacific basin (e.g., Goldfarb et al., 2007; Sun et al., 2007; Guo et al., 2013; Li and Santosh, 2013), although fluid and metal sources remain unclear. In addition, the specific deformation events in the late Mesozoic structural evolution of the craton margin are complex and still poorly understood (e.g., Mercier et al., 2007; Zhu et al., 2010).

Most workers agree that the Tan–Lu Fault, extending along much of eastern China and along the western side of the Jiaodong Peninsula, was characterized by sinistral strike–slip through the Late Jurassic (Wan, 1995; Zhang et al., 2001; Wan, 2004). This probably reflected oblique subduction of a Pacific plate below the craton and a resulting transpressive regime along the edge of the continent (Mao et al., 2010, 2011). By the start of the Cretaceous, a well recognized northwest–southeast extension affected all of eastern Asia. Crustal thinning and slab rollback during development of a more steeply-dipping orthogonal subduction region have been related to this major extensional event (e.g., Maruyama et al., 1997; Zhu et al., 2010). Consequences of the extension included widespread crustal melting, doming, moderately-dipping normal fault generation, and then metamorphic core complex unroofing with evolution of some fault segments to low-angle structures, such as defined by the history of the Linglong massif. Brittle deformation along a part of the Linglong detachment fault, and associated hydrothermal fluid flow, could simply relate to partial unroofing of the detachment into the more brittle crustal regime (e.g., Axen, 2004). Alternatively, northwest compression, perhaps associated with a major shift in the plate configuration in the Pacific basin (e.g., Goldfarb et al., 2007, 2013), may have reactivated the Zhaoping normal fault. Mercier et al. (2007) indicate such a compressional stress component during onset of northeast–southwest extension at ca. 127 Ma. This shift in the main extensional direction would have also caused sinistral strike–slip along the NE- and NNE-trending faults (Mercier et al., 2007), responsible for emplacement of the Guojialing plutons and fluid flow events along their margins during uplift (Fig. 8).

7. Conclusion

Previous workers have shown that most of the important gold deposits in the Zhaoyuan area of the Jiaodong gold province formed at ca. 120 ± 5 Ma. The $^{40}Ar/^{39}Ar$ dating results from this study provide the first precise age data on the Dayingezhuang gold deposit. The deposit is located along the Linglong detachment fault on the eastern margin to the Linglong metamorphic core complex. The data extend the oldest bound of the period of hydrothermal activity in the Jiaodong gold province to between 134 and 126 Ma. The older gold mineralization at Dayingezhuang suggests zones of brittle deformation along the southeastern margin of the massif may be equally prospective for large gold resources in the Zhaoyuan area.

Acknowledgments

We are very grateful to Associate Professor Roberto Weinberg of Monash University, who reviewed an early version of our manuscript with very constructive comments that greatly improved it, as well as comments from Stephanie Mills and Ryan Taylor. Thanks are given to Profs. Franco Pirajno, Shengrong Li and the Editor Prof. M. Santosh for their significant and constructive comments on this manuscript. This work was financially supported by the National Natural Science Foundation of China (Grant Nos. 41230311, 40872068, 40672064 and 40572063), the National Science and Technology Support Program (Grant No. 2011BAB04B09), the Program for New Century Excellent Talents (Grant No. NCET-09-0710), 111 Project (Grant No. B07011) and Changjiang Scholars and Innovative Research Team in University, the Ministry of Education, China (Grant No. IRT0755).

References

Ames, L., Zhou, G.Z., Xiong, B.C., 1996. Geochronology and isotopic character of ultrahigh-pressure metamorphism with implications for collision of the Sino–Korean and Yangtze cratons, central China. Tectonics 15, 472–489.
Axen, G.J., 2004. Mechanics of low-angle normal faults. In: Karner, G., Taylor, B., Driscoll, N., Kohlstedt, D.L. (Eds.), Rheology and Deformation in the Lithosphere at Continental Margins. Columbia University Press, New York, pp. 46–91.
Ayers, J.C., Dunkle, S., Gao, S., Miller, C.E., 2002. Constraints on timing of peak and retrograde metamorphism in the Dabieshan Ultrahigh-Pressure Metamorphic Belt, east-central China, using U–Th–Pb dating of zircon and monazite. Chemical Geology 186, 315–331.
Bohlke, J.K., 1988. Carbonate–sulfide equilibria and "stratabound" disseminated epigenetic gold mineralization: a proposal based on examples from Allegheny, California, USA. Applied Geochemistry 3, 499–516.
Charles, N., Gumiaux, C., Augier, R., Chen, Y., Zhu, R.X., Lin, W., 2011. Metamorphic core complexes vs. synkinematic plutons in continental extension setting: insights from key structures (Shandong Province, eastern China). Journal of Asian Earth Sciences 40, 261–278.
Charles, N., Augier, R., Gumiaux, C., Monie, P., Chen, Y., Faure, M., Zhu, R.X., 2013. Timing, duration, and role of magmatism in wide rift systems: insights from the Jiaodong Peninsula (China, East Asia). Gondwana Research 24, 412–428.
Chen, G.Y., Shao, W., Sun, D.S., 1989. Genetic Mineralogy of Gold Deposits in Jiaodong Region with Emphasis on Gold Prospecting. Chongqing Publish House, Chongqing 1–45 (in Chinese).
Chen, G.Y., Sun, D.S., Zhou, X.R., Gong, R.T., Shao, Y., 1993. Mineralogy of Guojialing Granodiorite and its Relationship to Gold Mineralization in the Jiaodong Peninsula. Chinese University of Geosciences Press, Beijing 230 (in Chinese with English abstract).
Chen, G.Y., Sun, D.S., Shao, Y., 1996. Typomorphic significance of accessory minerals of gold-hosting Kunyushan monzonitic granite in Jiaodong, China. Geosciences 10, 175–186 (in Chinese with English abstract).
Chen, J.F., Xie, Z., Li, H.M., Zhang, X.D., Zhou, T.X., Park, Y.S., Ahn, K.S., Chen, D.G., Zhang, X., 2003. U–Pb zircon ages for a collision-related K-rich complex at Shidao in the Sulu ultrahigh pressure terrane, China. Geochemical Journal 37, 35–46.

Chen, Y.J., Pirajno, F., Qi, J.P., 2005. Origin of gold metallogeny and sources of ore-forming fluids, Jiaodong Province, eastern China. International Geology Review 47, 530–549.

Davis, G.A., Lister, G.S., 1988. Detachment faulting in continental extension: perspectives from the southwestern U.S. Cordillera. Geological Society of America Special Paper, 218 133–159.

Davis, G.A., Qian, X., Zheng, Y., Yu, H., Wang, C., Mao, T.H., Gehrels, G.E., Muhammad, S., Fryxell, J.E., 1996. Mesozoic deformation and plutonism in the Yunmeng Shan: a Chinese metamorphic core complex north of Beijing, China. In: Yin, A., Harrison, T.A. (Eds.), The Tectonic Evolution of Asia. Cambridge University Press, New York, pp. 253–280.

Davis, G.A., Zheng, Y., Wang, C., Darby, B.J., Zhang, C., Gehrels, G.E., 2001. Mesozoic tectonic evolution of the Yanshan fold and thrust belt, with emphasis on Hebei and Liaoning provinces, northern China. In: Hendrix, M.S., Davis, G.A. (Eds.), Paleozoic and Mesozoic tectonic evolution of central and eastern Asia: from continental assembly to intracontinental deformation. Geology Society of America memoir, 194, pp. 171–194.

Deng, J., Xu, S.L., Fang, Y., Wang, L., Zhou, X.Q., 1996. Structural System and Gold Ore-forming Dynamics in the Northwestern Part of Jiaodong Peninsula. Geological Press, Beijing 1–98 (in Chinese with English abstract).

Deng, J., Zhai, Y.S., Yang, L.Q., Xiao, R.G., Sun, Z.S., 1999. Tectonic evolution and dynamics of metallogenic system — an example from the gold ore deposits concentrated area in Jiaodong, Shandong, China. Earth Sciences Frontiers 6, 315–323 (in Chinese with English abstract).

Deng, J., Yang, L.Q., Sun, Z.S., Wang, J.P., Wang, Q.F., Xin, H.B., Li, X.J., 2003. A metallogenic model of gold deposits of the Jiaodong granite–greenstone belt. Acta Geologica Sinica 77, 537–546.

Deng, J., Yang, L.Q., Ge, L.S., Wang, Q.F., Zhang, J., Gao, B.F., Zhou, Y.H., Jiang, S.Q., 2006. Research advances in the Mesozoic tectonic regimes during the formation of Jiaodong ore cluster area. Progress in Nature Sciences 16, 777–784.

Deng, J., Chen, Y.M., Liu, Q., Yang, L.Q., 2010. The Gold Metallogenic System and Mineral Resources Exploration of Sanshandao Fault Zone. Geological Press, Shandong Province, Beijing 1–371 (in Chinese).

Faure, M., Lin, W., Monie, P., Breton, N.L., Poussineau, S., Panis, D., Deloule, E., 2003. Exhumation tectonics of the ultrahigh-pressure metamorphic rocks in the Qinling orogen in east China: new petrological–structural–radiometric insights from the Shandong Peninsula. Tectonics 22, 1018–1040.

Fu, Y.L., Lu, X.Q., Zhang, S.H., Wang, L.T., 1987. $^{40}Ar/^{39}Ar$ dating techniques and age determination of some geological samples. Bulletin of the Institute of Geology, CAGS 17, 85–107 (in Chinese with English abstract).

Goldfarb, R.J., Groves, D.I., Gardoll, D., 2001. Orogenic gold and geologic time: a global synthesis. Ore Geology Reviews 18, 1–75.

Goldfarb, R.J., Hart, C.J.R., Davis, G., Groves, D.I., 2007. East Asian gold: deciphering the anomaly of Phanerozoic gold in Precambrian cratons. Economic Geology 102, 341–346.

Goldfarb, R.J., Taylor, R.D., Collins, G.S., Goryachev, N.A., Orlandini, O.F., 2013. Phanerozoic continental growth and gold metallogeny of Asia. Gondwana Research. http://dx.doi.org/10.1016/j.gr.2013.03.002.

Guo, Z.Y., Sun, X.Z., He, X.P., Chu, Y.l, 1990. Ore-controlling structure geochemistry and prospecting direction of gold deposits in Jiaodong area. Institute of Geological Sciences Research of Shandong Province, China 1–293 (Unpublished (in Chinese)).

Guo, J.H., Zhai, M.G., Ye, K., Liu, W.J., Cong, B.L., 2002. Petrochemistry and geochemistry of HP metabasites from Haiyangsuo in Sulu UHP belt of eastern China. Science in China Series D: Earth Sciences 32, 394–404.

Guo, J.H., Chen, F.K., Zhang, X.M., Siebel, W., Zhai, M.G., 2005. Evolution of syn-to post-collisional magmatism from North Sulu UHP belt, eastern China: zircon U–Pb geochronology. Acta Petrologica Sinica 21, 1281–1301 (in Chinese with English abstract).

Guo, P., Santosh, M., Li, S.R., 2013. Geodynamics of gold metallogeny in the Shandong Province, NE China: a geological and geophysical perspective. Gondwana Research. http://dx.doi.org/10.1016/j.gr.2013.02.004.

Hacker, B.R., Ratschbacher, L., Webb, L.E., Walker, D., Dong, S.W., 1998. U–Pb zircon ages constrain the architecture of the ultrahigh-pressure Qinling–Dabie Orogen, China. Earth and Planetary Science Letters 161, 215–230.

Hames, W.E., Bowring, S.A., 1994. An empirical evaluation of the argon diffusion geometry in muscovite. Earth and Planetary Science Letters 124, 161–169.

Harrison, T.M., Celerier, J., Aikman, A.B., Hermann, J., Heizler, M.T., 2009. Diffusion of 40Ar in muscovite. Geochimica et Cosmochimica Acta 73, 1039–1051.

Hou, M.L., Jiang, Y.H., Jiang, S.Y., Ling, H.F., Zhao, K.D., 2007. Contrasting origins of late Mesozoic adakitic granitoids from the northwestern Jiaodong Peninsula, East China: implications for crustal thickening to delamination. Geological Magazine 144, 619–631.

Hu, S.L., Wang, S.S., Sang, H.Q., Qiu, J., Zhang, R.H., 1987. Isotopic ages of Linglong and Guojialing batholiths in Shandong Province and their geological implication. Acta Petrologica Sinica 3, 83–89 (in Chinese with English abstract).

Hu, F.F., Fan, H.R., Yang, J.H., Wan, Y.S., Liu, D.Y., Zhai, M.G., Jin, C.W., 2004. Hydrothermal U–Pb zircon Shrimp dating ore-forming age of the lode gold–quartz–sulphide veins in Rushan, Jiaodong Peninsula. Chinese Science Bulletin 49, 1191–1198.

Jahn, B.M., Liu, D.Y., Wan, Y.S., Song, B., Wu, J.S., 2008. Archean crustal evolution of the Jiaodong Peninsula, China, as revealed by zircon SHRIMP geochronology elemental and Nd-isotope geochemistry. American Journal of Science 308, 232–269.

Lanphere, M.A., Baadsgaard, H., 1997. The Fish Canyon Tu: a standard for geochronology. AGU Abstracts with Program 78 (17), S326.

Li, S.G., Chen, Y.Z., 1994. U–Pb zircon ages of amphibolite from the Haiyangsuo area, eastern Shandong province. Acta Geoscientia Sinica 1–2, 37–42 (in Chinese with English abstract).

Li, S.R., Santosh, M., 2013. Metallogeny and craton destruction: records from the North China Craton. Ore Geology Reviews. http://dx.doi.org/10.1016/j.oregeorev.2013.03.002.

Li, Z.L., Yang, M.Z., 1993. The Geology–Geochemistry of Gold Deposits in Jiaodong Region. Science and Technology Press, Tianjing 1–293 (in Chinese with English abstract).

Li, J.W., Vasconcelos, P.M., Zhang, J., Zhou, M.F., Zhang, X.J., Yang, F.H., 2003. $^{40}Ar/^{39}Ar$ constraints on a temporal link between gold mineralization, magmatism, and continental margin transtension in the Jiaodong gold province, eastern China. Journal of Geology 111, 741–751.

Li, J.W., Vasconcelos, P.M., Zhou, M.F., Zhao, X.F., Ma, C.Q., 2006. Geochronology of the Pengjiakuang and Rushan gold deposits, eastern Jiaodong gold province, northeastern China: implications for regional mineralization and geodynamic setting. Economic Geology 101, 1023–1038.

Li, Q.L., Chen, F.K., Yang, J.H., Fan, H.R., 2008. Single grain pyrite Rb–Sr dating of the Linglong gold deposit, eastern China. Ore Geology Reviews 34, 263–270.

Lin, W.W., Yin, X.L., 1998. The forming physicochemical conditions of Linglong granitic complex and its geological significance. Acta Geoscientia Sinica 19, 40–49 (in Chinese with English abstract).

Lin, W., Faure, M., Monie, P., Scharer, U., Panis, D., 2008. Mesozoic extensional tectonics in eastern Asia: the South Liaodong Peninsula metamorphic core complex (NE China). Journal of Geology 116, 134–154.

Liou, J.G., Tsujimori, T., Chu, W., Zhang, R.Y., Wooden, J.L., 2006. Protolith and metamorphic ages of the Haiyangsuo Complex, eastern China: a non-UHP exotic tectonic slab in the Sulu ultrahigh-pressure terrane. Mineral and Petrology 88, 207–226.

Liu, S., Hu, R.Z., Zhao, J.H., Feng, C.X., 2004. K–Ar geochronology of Mesozoic mafic dikes in Shandong Province, eastern China: implications for crustal extension. Acta Geologica Sinica 78, 1207–1213.

Lu, S.N., 1998. Geochronology and Sm–Nd isotopic geochemistry of Precambrian crystalline basement in eastern Shandong Province. Earth Sciences Frontiers 5, 275–283 (in Chinese with English abstract).

Lu, K.Z., Dai, J.S., 1994. Evolution of Jiaolai Pull-apart Basin. Petroleum University Press, Dongying 1–174 (in Chinese).

Lu, G.X., Kong, Q.C., 1993. Geology of Linglong–Jiaojia Type of Gold Deposits in Jiaodong Area. Science Press, Beijing 1–253 (in Chinese with English abstract).

Luo, Z.K., Miao, L.C., 2002. Granites and Gold Deposits in Zhaoyuan–Laizhou Area. Metallurgical Industry Press, Eastern Shandong Province, Beijing 84–117 (in Chinese with English abstract).

Luo, W.C., Wu, Q.S., 1987. Determination of gold metallogenic age in Jiaodong with the application of alteration minerals. Chinese Science Bulletin 16, 1245–1248 (in Chinese).

Mao, J.W., Wang, Y.T., Zhang, Z.H., Yu, J.J., Niu, B.G., 2003. Geodynamic settings of Mesozoic large-scale mineralization in North China and adjacent areas: implication from the highly precise and accurate ages of metal deposits. Science in China Series D: Earth Sciences 46, 838–851.

Mao, J.W., Xie, G.Q., Pirajno, F., Ye, H.S., Wang, Y.B., Li, Y.F., Xiang, J.F., Zhao, H.J., 2010. Late Jurassic–Early Cretaceous granitoid magmatism in Eastern Qinling, central-eastern China: SHRIMP zircon U–Pb ages and tectonic implications. Australian Journal of Earth Sciences 57, 51–78.

Mao, J.W., Pirajno, F., Cook, N., 2011. Mesozoic metallogeny in East China and corresponding geodynamic settings — an introduction to the special issue. Ore Geology Reviews 43, 1–7.

Maruyama, S., Isozaki, Y., Kimura, G., Terbayashi, M.C., 1997. Paleogeographic maps of the Japanese islands: plate tectonic synthesis from 750 Ma to the Present. Island Arc 121–142.

McDougall, I., Harrison, T.M., 1999. Geochronology and Thermochronology by the $^{40}Ar/^{39}Ar$ Method. Oxford University Press, New York 269.

Mercier, J., Hou, M., Vergely, P., Wang, Y., 2007. Structural and stratigraphical constraints on the kinematics history of the southern Tan–Lu Fault zone during the Mesozoic Anhui Province, China. Tectonophysics 439, 33–66.

Passchier, C.W., Trouw, R.A., 2005. Microtectonics, 2nd edition. Springer, Berlin 1–289.

Qiu, Y.M., Groves, D.I., McNaughton, N.J., Wang, L.G., Zhou, T.H., 2002. Nature, age and tectonic setting of granitoid-hosted, orogenic gold deposits of the Jiaodong Peninsula, eastern North China Craton, China. Mineralium Deposita 37, 283–305.

Ren, F.L., Liu, Z.Q., Qiu, L.G., Han, L.G., Zhang, Y.Q., Cao, Z.X., 2008. The prototype character of Jiaolai Basin in Cretaceous Laiyang period. Acta Sedimentologica Sinica 26, 221–233 (in Chinese with English abstract).

Snee, L.W., Sutter, J.F., Kelly, W.C., 1988. Thermochronology of economic mineral deposits — dating the stages of mineralization at Panasqueira, Portugal, by high precision ^{40}Ar–^{39}Ar age spectrum techniques on muscovite. Economic Geology 83, 335–354.

Song, M.C., Wang, P.C., Liang, B.Q., 2003. Regional Geology of Shandong Province. Shandong Cartographic Press, Jinan 25–720.

Spencer, J.E., 1984. Role of tectonic denudation in warping and uplift of low-angle normal faults. Geology 12, 95–98.

Sun, F.Y., Shi, Z.L., Feng, B.Z., 1995. The Geology of Gold Deposits in Jiaodong and the Petrogenesis and Metallogenesis of Mantle-derived C–H–O Fluids. People's Press of Jilin, Changchun 1–70 (in Chinese).

Sun, W.-D., Ding, X., Hu, Y.-H., Li, X.-H., 2007. The golden transformation of the Cretaceous plate subduction in the west Pacific. Earth and Planetary Science Letters 262, 533–542.

Tang, J., Zheng, Y.F., Wu, Y.B., Gong, B., Liu, X.M., 2007. Geochronology and geochemistry of metamorphic rocks in the Jiaobei terrane: constraints on its tectonic affinity in the Sulu orogen. Precambrian Research 152, 48–82.

Tang, J., Zheng, Y.F., Wu, Y.B., Gong, B., Zha, X.P., Liu, X.M., 2008. Zircon U/Pb age and geochemical constraints on the tectonic affinity of the Jiaodong Terrane in the Sulu orogen, China. Precambrian Research 161, 389–418.

Teng, P.D., 1985. Discussion on the three basic problems of controlling the gold deposits in the Zhaoyuan–Yexian region. Geology in Shandong 1, 83–91 (in Chinese with English abstract).

Wallis, S., Enami, M., Banno, S., 1999. The Sulu UHP terrane: a review of the petrology and structural geology. International Geology Review 41, 906–920.

Wan, T.F., 1995. Evolution of Tancheng–Lujiang Fault zone and paleostress fields. Earth Science: Journal of China University of Geosciences 20, 526–534 (in Chinese with English abstract).

Wan, T.F., 2004. China Tectonics Framework. Geological Press, Beijing 1–387 (in Chinese).

Wang, P.C., An, Y.H., 1996. Main achievement and progress of the basic geological research over last ten years in eastern Shandong region. Shandong Geology 12, 8–23 (in Chinese with English abstract).

Wang, K.H., Qiou, Y.S., Cui, K.Y., Han, S.Z., 1984. The control conditions of the gold deposits in Zhaoyuan–Yexian area, Shandong. Bulletin of Shenyang Institute of Geology and Mineral Resources, Chinese Academy of Geological Sciences 9, 10–30 (in Chinese with English abstract).

Wang, L.G., Qiu, Y.M., McNaughton, N.J., Groves, D.I., Luo, Z.K., Huang, J.Z., Miao, L.C., Liu, Y.K., 1998. Constraints on crustal evolution and gold metallogeny in the northwestern Jiaodong Peninsula, China, from SHRIMP U–Pb zircon studies of granitoids. Ore Geology Reviews 13, 275–291.

Wang, Y.W., Zhu, F.S., Gong, R.T., 2002. Study on the metallogenic chronology of gold deposits in Jiaodong gold concentration zone. Gold Geology 8, 48–55 (in Chinese with English abstract).

Xu, B., 1999. Geologic and Geochemical Characteristics of Dayingezhuang Gold Deposit in Shandong Peninsula, China. (Ph.D. thesis) Technical School of Tokyo University 1–139 (in Japanese with English abstract).

Xu, J.W., Zhu, G., Tong, W.X., Cui, K.R., Liu, Q., 1987. Formation and evolution of the Tancheng–Lujiang wrench fault system: a major shear system to the northwest of the Pacific Ocean. Tectonophysics 134, 273–310.

Yang, J.H., Zhou, X.H., 2001. Rb–Sr, Sm–Nd, and Pb isotope systematics of pyrite: implications for the age and genesis of lode gold deposits. Geology 29, 711–714.

Yang, J.H., Zhou, X.H., Chen, L.H., 2000. Dating of gold mineralization for superlarge altered tectonite-type gold deposits in northwestern Jiaodong Peninsula and its implications for gold metallogeny. Acta Petrologica Sinica 16, 454–458 (in Chinese with English abstract).

Yang, J.H., Wu, F.Y., Wilde, S.A., 2003. A review of the geodynamic setting of large-scale late Mesozoic gold mineralization in the North China Craton: an association with lithospheric thinning. Ore Geology 23, 123–152.

Yang, J.H., Zhong, S.L., Wilder, S.A., Wu, F.Y., Chu, M.F., Lo, C.H., Fan, H.R., 2005. Petrogenesis of post-orogenic syenites in the Sulu orogenic belt, East China: geochronology, geochemical and Nd–Sr isotopic evidence. Chemical Geology 214, 99–125.

Yang, L.Q., Deng, J., Wang, Q.F., Zhou, Y.H., 2006. Coupling effects on gold mineralization of deep and shallow structures in the northwestern Jiaodong Peninsula, eastern China. Acta Geologica Sinica 80, 400–411.

Yang, L.Q., Deng, J., Ge, L.S., Wang, Q.F., Zhang, J., Gao, B.F., Jiang, S.Q., Xu, H., 2007a. Metallogenic age and genesis of gold ore deposits in Jiaodong Peninsula, eastern China. A regional review. Progress in Nature Sciences 17, 138–143.

Yang, L.Q., Deng, J., Zhang, J., Wang, Q.F., Ge, L.S., Zhou, Y.H., Guo, C.Y., Jiang, S.Q., 2007b. Preliminary studies of fluid inclusions in Damoqujia gold deposit along Zhaoping Fault zone, Shandong province, China. Acta Petrologica Sinica 23, 153–160.

Yang, L.Q., Deng, J., Zhang, J., Guo, C.Y., Gao, B.F., Gong, Q.J., Wang, Q.F., Jiang, S.Q., Yu, H.J., 2008. Decrepitation thermometry and compositions of fluid inclusions of the Damoqujia gold deposit, Jiaodong gold province, China: implications for metallogeny and exploration. Journal of China University of Geosciences 19, 378–390.

Yang, L.Q., Deng, J., Guo, C.Y., Zhang, J., Jiang, S.Q., Gao, B.F., Gong, Q.J., Wang, Q.F., 2009. Ore-forming fluid characteristics of the Dayingezhuang gold deposit, Jiaodong gold province, China. Resource Geology 59, 182–195.

Yang, Q.Y., Santosh, M., Shen, J.F., Li, S.R., 2013. Juvenile vs. recycled crust in NE China: zircon U–Pb geochronology, Hf isotope and an integrated model for Mesozoic gold mineralization in the Jiaodong Peninsula. Gondwana Research. http://dx.doi.org/10.1016/j.gr.2013.06.003.

Yao, F.L., Liu, L.D., Kong, Q.C., Gong, R.T., 1990. Gold Lodes in the Northwestern Part of the Jiaodong Peninsula (in Chinese). Science & Technology Press, Changchun 1–234.

Ye, K., Cong, B.L., Hirajima, T., Banno, S., 1999. Transformation from granulite to transitional eclogite at Haiyangsuo, Rushan Country, eastern Shandong Peninsula: the kinetic process and tectonic implications. Acta Petrologica Sinica 15, 21–36 (in Chinese with English abstract).

Zen, E.A., Hammarstrom, J.M., 1984. Magmatic epidote and its petrologic significance. Geology 12, 515–518.

Zeng, L.S., Chen, J., Chen, Z.Y., Liu, J., Liang, F.H., Gao, L.E., 2007. Emplacement depth of the Shidao granitic complex and the rapid exhumation of the Sulu ultrahigh pressure rocks: new constraints on the mechanisms for rapid exhumation. Acta Petrologica Sinica 23, 3171–3179 (in Chinese with English abstract).

Zhai, M.G., Santosh, M., 2013. Metallogeny of the North China Craton: link with secular changes in the evolving Earth. Gondwana Research 24, 275–297.

Zhai, M.G., Cong, B.L., Guo, J.H., Liu, W.J., Li, Y.G., Wang, Q.C., 2000. Sm–Nd geochronology and petrography of garnet pyroxene granulites in the northern Sulu region of China and their geotectonic implication. Lithos 52, 23–33.

Zhai, Y.S., Deng, J., Tang, Z.L., Xiao, G., Song, H.L., Peng, R.M., Sun, Z.S., Wang, J.P., Xiang, Y.C., Huang, H.S., Zhang, Z.W., Yang, L.Q., Bai, Y.L., Chen, C.X., Ding, S.J., Wang, Q.F., Hu, L., Xu, Z.G., Miao, L.C., Su, S.G., Li, Q.Z., Gong, Y.F., 2002. Metallogenic Systems of Paleocontinental Margin. Geological Publishing House, Beijing 1–416 (in Chinese with English abstract).

Zhang, T., Zhang, Y.Q., 2007. Geochronological sequence of Mesozoic intrusive magmatism in Jiaodong Peninsula and its tectonic constraints. Geological Journal of China Universities 13, 323–336 (in Chinese with English abstract).

Zhang, Z.H., Zhang, J.X., Ye, S.Z., 1994. The Isotopic Age of Gold Deposits in Jiaodong Peninsula. Seismology Press, Beijing 1–56 (in Chinese).

Zhang, C.H., Song, H.L., Wang, G.H., Yan, D.P., Sun, W.H., 2001. Mesozoic dextral strike–slip structural system in middle segment of intraplate Yanshan orogenic belt, Northern China. Earth Science: Journal of China University of Geosciences 20, 526–534 (in Chinese with English abstract).

Zhang, L.C., Sheng, Y.C., Li, H.M., Zeng, Q.D., Li, G.M., Liu, T.B., 2002. Helium and argon isotopic compositions of fluid inclusions and tracing to the source of ore-forming fluids for Jiaodong gold deposits. Acta Petrologica Sinica 18, 559–565.

Zhang, X.O., Cawood, P.A., Wilde, S.A., Liu, R.Q., Song, H.L., Li, W., Snee, L.W., 2003. Geology and timing of mineralization at the Cangshang gold deposit, Northwestern Jiaodong Peninsula, China. Mineralium Deposita 38, 141–153.

Zhang, Y.Q., Dong, S.W., Shi, W., 2003. Cretaceous deformation history of the middle Tan–Lu Fault zone in Shandong Province, eastern China. Tectonophysics 363, 243–258.

Zhang, H.Y., Hou, Q.L., Cao, D.Y., 2006. Study on Mesozoic thrust and nappe tectonics in Eastern Jiaodong. Science in China Series D: Earth Sciences 36, 497–506 (in Chinese).

Zhang, Y.Q., Li, J.L., Zhang, T., Yuan, J.Y., 2007. Late Mesozoic kinematic history of the Muping–Jimo Fault zone in Jiaodong Peninsula, Shandong province, East China. Geological Review 53, 289–300 (in Chinese with English abstract).

Zhou, J., 1995. On genesis of gold deposits in Zhaoye District, Shandong. Journal of Shenyang Institute of Gold Technology 14, 8–15 (in Chinese with English abstract).

Zhou, T.H., Lu, G.X., 2000. Tectonics, granitoids and Mesozoic gold deposits in East Shandong, China. Ore Geology Review 16, 71–90.

Zhu, G., Niu, M.L., Xie, C.L., Wang, Y.S., 2010. Sinistral to normal faulting along the Tan–Lu Fault zone: evidence for geodynamic switching of the east China continental margin. Journal of Geology 118, 277–293.